PEOPLE'S DEMOCRATIC REPUBLIC OF ALGERIA

MINISTRY OF HIGHER EDUCATION AND SCIENTIFIC RESEARCH

LAARBI TEBESSI UNIVERSITY OF TEBESSA

FACULTY OF EXACT SCIENCES AND THE SCIENCES OF NATURE AND LIFE

DEPARTMENT OF MATTER SCIENCES

THESIS of MASTER

Specialty: **Physics of materials**

Effect of Cr doping on optical and electrical properties of CuO thin films deposited by spray pyrolysis technique

Presented by:

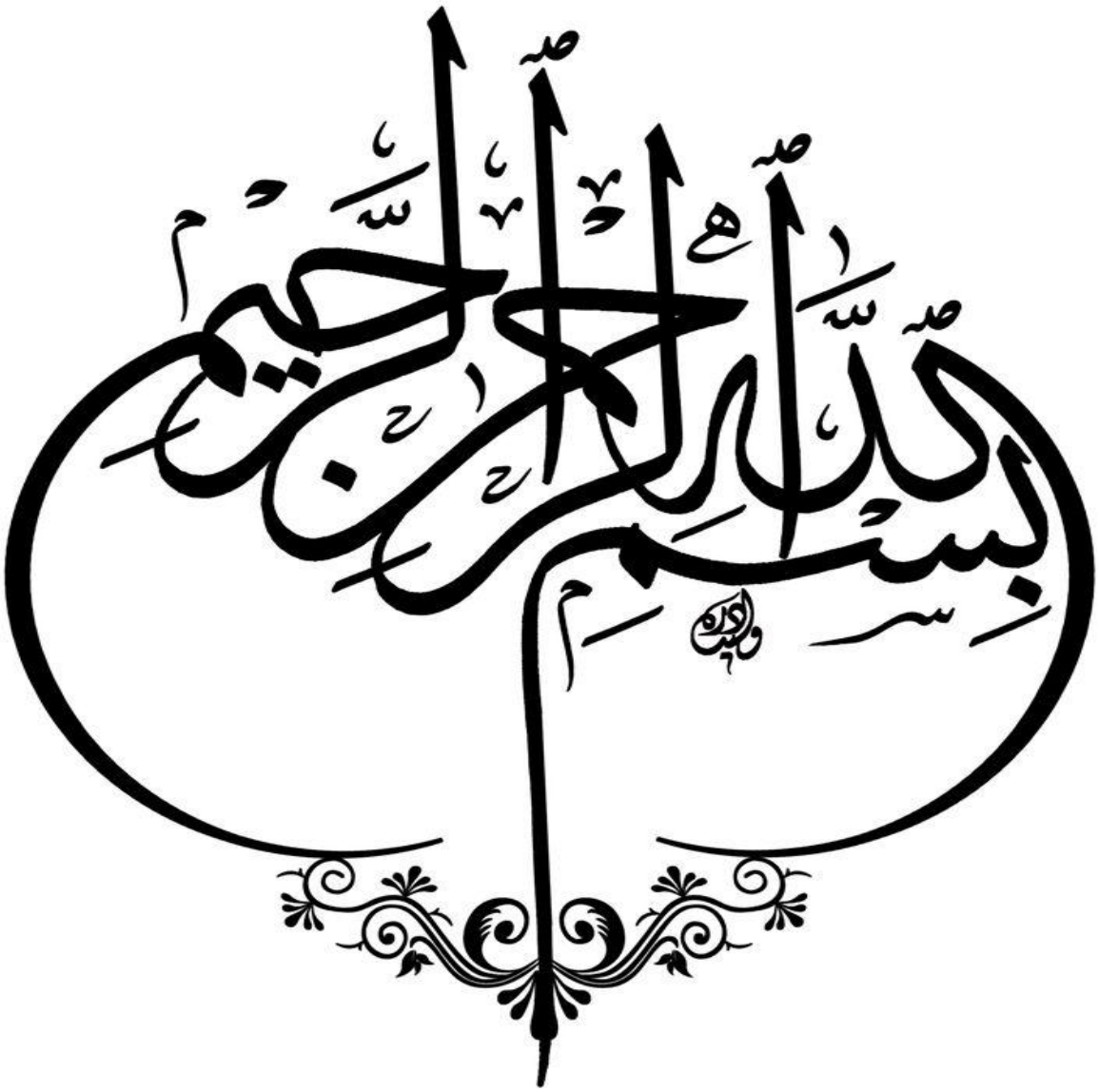
Assel Anfel **Merahi Rayene**

Members of jury:

Dr. Bouhlal Mouna	**Larbi Tebessi University**	**President**
Dr. Labidi Herissi	**Larbi Tebessi University**	**Supervisor**
Dr. Taki-eddine Kiraouani	**Larbi Tebessi University**	**Examiner**

date?

University season: **2024/2025**



«يَرْفَعِ اللَّهُ الَّذِينَ آمَنُوا مِنكُمْ وَالَّذِينَ أُوتُوا الْعِلْمَ دَرَجَاتٍ»

المجادلة – الآية 11

Acknowledgements

Primarily, I would thank Allah for being able to complete this project with success.

First of all,we would like to extend our sincere thanks and appreciation to **Mr. Labidi HERISSI**, Senior Lecturer at Larbi Tebessi University of Tebessa, for his exceptional supervision, valuable advice, and continuous guidance throughout this work. We were truly fortunate to have him as our supervisor; his support was instrumental in the successful completion of this thesis.

We also express our heartfelt thanks to the jury members: Professor **BOUHLAL Mouna, Mr.Taki-eddine Kiraouani**, Senior Lecturer at Larbi Tebessi University of Tebessa, for their interest in our research, their presence at our defense, and their constructive suggestions that enriched this work.

Our gratitude also goes to Professor Lazher HADJERIS, Director of the Laboratory of Materials and Structures of Electromechanical Systems and Their Reliability at Larbi Ben MHidi University of Oum El Bouaghi, and Professor Abdelkarim GUOUSSMIA, Director of the Laboratory of Organic Materials and Heterochemistry at Larbi Tébessi University of Tebessa, for their warm welcome and support.

We would also like to thank all the faculty members at Larbi Tébessi University of Tébessa, for their high-quality teaching and ongoing support throughout our academic journey.

We are deeply grateful to our brothers and sisters for their constant encouragement and support, and to our friends and fellow students, particularly our classmates in the second year of the Master's program in Materials Physics, for their good spirit and camaraderie.

Finally, to all those who contributed, directly or indirectly, to the realization of this thesis, we extend our warmest thanks and appreciation. May Allah reward you all.

اهداء

الحمد لله حمدًا يليقُ بجلاله وامتنانًا، ماكنتُ لأصل لهذا لولا فضل الله، فالحمد لله على البدء، وعلى الختام...

وأُخِتر دَعْوَاهُمْ أنِ الحمدُ للهِ ربِّ العالمين

أهدي هذا النجاح أولا إلى نفسي الطموحة جداً ، واني استمريت بالسعي رغم ثقل الطريق و كثرة عثراته فخورة بنفسي و جدا...

" فاللهم لا تجعله اخر عهدي من العلم و اجعلها خير بداية لطريق اعظم اللهم بارك لنا في عملنا و انفعنا بما علمتنا"

اهدي ثواب هذا البحث الى من لا ينفصل اسمه عن اسمي الرجل العظيم، الذي علمني ان الدنيا كفاح و سلاحها العلم و

المعرفة ، مصدر قوتي و فخري و داعمي الأول لطالما عاهدته بهذا النجاح و ها انا اتممت وعدي

(بابا الغالي حفظه الله)

الى عزيزة القلب من مدت لي يدها أوقات الضعف و راهنت على نجاحي و ضلت دعواتها تضم اسمي، جوهرتي النادرة

منبع الحنان و نبع العطاء

(والدتي الغالية)

الى من شددت عضدي بهما ، السند والكتف الثابت الذين اذا مالت الدنيا لا يميلون اخواي

(انس و ايهم)

الى امان ايامي ، صديقتي الأولى و خيرة ايامي و صفوتها قرة العين اختي

(اسراء)

الى سكر عالمي...

صديقة المواقف لا السنين شريكة الدرب الطويل (ريان)

انفال

إهداء

أُهدي هذا العمل المتواضع إلى من بذل الغالي والنفيس من أجلي، إلى من شرب الكأس فارغًا ليمنحني قطرة حب، إلى من تحمل المشقة ليُمهّد لي طريق العلم والمعرفة... إلى والديّ العزيزين، وإلى والدتي الثانية.

إلى من كان دعاؤهما سببًا في توفيقي، وحنانهما بلسمًا لكل جراحي، إلى من كانت قلوبهما مصدر الأمان، إلى والدتي الأولى والثانية، سندي وقوتي وملجأي بعد الله، إلى من جعل الله الجنة تحت قدميهما، إلى من أكرمتاني بحنانهما وتفانيهما، أهدي تخرجي عرفانًا وامتنانًا لا يفيه التعبير.

كما أُهديه إلى إخوتي الأعزاء: أكرم، شيماء، روميساء، مروى، رندة، وإلى جميع أفراد أسرتي الكريمة.

ولا أنسى أن أُعبر عن امتناني لصديقاتي العزيزات: انفال، يسرى، هالة، وصديقتي وحبيبتي لوجين، فوجودكن كان دعمًا لا يُقدّر بثمن.

وأخيرًا، أهدي تخرجي إلى والدتي الثانية، راجيةً من الله عزوجل أن يرزقها الشفاء العاجل والصحة الدائمة.

ريان

Table of content

List of figures	V
List of tables	VIII
List of symbols	IX
List of abbreviations	X
General introduction	01
Chapter I: Overview on copper oxide thin film	
I.1. Overview on thin film	3
I.2. Thin film deposition techniques	3
I.2.1. Physical deposition Methods	4
I.2.1.1. Stages of formation of thin films by physical methods	4
I.2.1.2. Vacuum evaporation techniques	7
A. Thermal evaporation technique	7
B. Laser beam evaporation	8
C. Molecular beam epitaxy	8
D. Electron beam heating	9
I.2.1.3. Sputtering technique	10
I.2.2. Chemical deposition Methods	10
I.2.2.1. Chemical vapor deposition	10
A. Plasma enhanced chemical vapor deposition	12
B. Metal-organic chemical vapor deposition	12
C. Ultra-high vacuum chemical vapor deposition	13
I.2.2.2. Chemical solution deposition	13
A. Sol–Gel technique	13

B. Chemical bath deposition technique	14
C. Electrodeposition	15
D. Spray pyrolyse	16
I.3. Transparent conductive oxides	16
I.3.1. Definition	16
I.3.2. Metal oxides	17
I.4. Copper oxide: properties and applications	17
I.4.1.Formation of copper-based oxides	17
I.4.2. Cuprous oxide Cu2O	18
• I.4.2.1. Crystallographic structure	18
• I.4.2.2. Optical properties	20
• I.4.2.3. Electrical properties of Cu_2O	21
I.4.2. cupric oxide (CuO)	21
I.4.2.1.Crystallographic structure	21
I.4.2.2. Optical properties of copper (II) oxide	23
I.4.2.3. Electrical properties of CuO	25
I.4.3.Applications of thin copper oxide films	25
Chapter II :Elaboration of copper oxide thin films	
Part one : Ultrasonic spray pyrolysistechnique technique	26
II.1.The choice of ultrasonic spray pyrolysis technique	26
II.1.1.Principle of thermal decomposition deposition technique	26
II.1.2. The advantages of spray pyrolysis technique	27
II.1.3. Factors affecting thin film preparation by ultrasonic spray pyrolysis technique	27
A. Atomization rate and droplet size	27

B. Thermal effects of the substrate on droplets	28
C. Effect of deposit time	29
D. Effect of the nozzle-substrate distance	29
II.2. Experimental procedure	30
II.3. Followed equipmen	30
II.4. Stages of preparation thin films	32
II.5. Preparation of deposition solutions	33
a.Preparation of copper(II) chloride colution	33
b. Preparation of chromium chloride solution	34
c. Preparation of precursor solution	36
II.6. Deposition of thin film	36
II.7.Annealing of deposited samples	37
.Part two: Characterization techniques of thin films	39
II.1. Optical characterization of thin films	39
II.1.1.Ultraviolet-visible spectroscopy	39
II.1.1.1. Determination of film thickness and refractive index	41
II.1.1.2. Determination of absorption coefficient	41
II.1.1.3.Determination of optical band gap	42
II.1.1.4. Determination of Urbach Energy	44
II.2. Electrical characterization of thin films	44
Chapter III : Results and discussion	
III.1. Photos of CuO :Cr samples	47
III.2 Optical characterizations	48
III.2.1. Effect of Cr-doping and annealing on the optical transmittance of CuO samples	48
III.2.2.The effect of doping and annealing on the thickness of CuO:Cr film	50

III.2.3.Effect of chromium doping and annealing on the optical absorption of CuO thin films	51
III.2.4. The effect of doping and annealing on the Urbach energy of CuO:Cr	52
III.2.5.The effect of doping and annealing on the optical band gap of CuO:Cr	53
III.2.6. The effect of doping and annealing on the refractive index of CuO:Cr	55
III.3. Electrical characterizations	56
III.3.1. Effect of chromium doping and annealing on the electrical conductivity of Cu_xO	56
General conclusion	59
References	60

Figure No.	Title	Page
I.1	Thin film deposition techniques	**4**
I.2	A schematic diagram illustrating the nucleation stage of thin film deposition	**5**
I.3	A schematic illustrating the coalescence stage	**5**
I.4	A diagram illustrating the stages of coalescence and growth of thin fims	**6**
I.5	Growth modes of thin films	**6**
I.6	Thermal evaporation technique machine and its diagram	**7**
I.7	Pulsed laser deposition machine and its diagram	**8**
I.8	. Molecular beam epitaxy (MBE) machine and its diagram	**9**
I.9	Electron beam heating machine and its diagram	**9**
I.10	Sputtering technique machine and its diagram	**10**
I.11	CVD steps thin film formation	**11**
1.12	Diagram and machine PECVD	**12**
I.13	MOCVD system diagram	**13**
I.14	UHV-CVD system diagram	**13**
I.15	Dip coating basic process	**14**
I.16	Spin-Coating basic process	**14**
I.17	Chemical bath deposition technique	**15**
I.18	Electrodeposition diagram	**15**
I.19	Pyrolysis spraying diagram	**16**
I.20	Cuprous oxide "Cu_2O" **(a)** in the form of natural cuprite and **(b)** powder	**19**

I.21	Crystallographic structure of Cu_2O	**19**
I.22	Copper oxide "CuO" in the form of natural tenorite **(a)** and powder **(b)**	**22**
I.23	Structure cristalline de CuO **(a)** une cellule unitaire **(b)** quatre cellules unitaires	**22**
I.24	The Bandgap of CuO thin film	**24**
I.25	The UV-visible absorption spectra of CuO thin film	**24**
II.1	Droplet size effect on the formation of thin films	**28**
II.2	Thermal effects of the substrate on droplets	**29**
II.3	Effect of nozzle-substrate distance on film elaboration	**30**
II.4	Pyrolysis spraying device	**31**
II.5	The schematic experimental set up of the spray pyrolysis system	**31**
II.6	Glass microscope slides (substrates)	**32**
II.7	Substrate cleaning steps with some used tools	**33**
II.8	Copper(II) chloride dihydrate	**33**
II.9	Preparation of copper(II) chloride dihydrate solution	**34**
II.10	Chromium chloride hexahydrate	**35**
II.11	Preparation of chromium chloride hexahydrate solution	**35**
II.12	Deposition of thin film; **a.** doped solutions, **b.** the syringe, **c.** spraying the solution	**37**
II.13	Picture of an electric heating device	**38**
II.14	Principe of measure the transmission UV-Vis-NIR	**40**
I.15	Experimental device for UV-Vis-NIR spectroscopy	**40**
I.16	Transmittance spectrum of CuO:Cr (9 at.%) thin film after annealing at 350°C	**40**

I.17	Explanation of band gap	**43**
I.18	Band gap determination of CuO:Cr film before annealing	**43**
I.19	Urbach energy determination of CuO:Cr film before annealing	**44**
I.20	Four-point probe + keitheley 2400 Source Meter	**45**
I.21	Diagram representative of the principle of the four-point probes method	**46**
III.1	Optical transmittance spectra of CuO samples doped with different concentrations of Cr **(a):** before annealing **(b):** after annealing	**48**
III.2	Effect of annealing on the optical transmittance of glass and Cr_2O_3 sample	**49**
III.3	Optical transmittance spectra of CuO:Cr thin films at different percentage of Cr **(a):** before annealing **(b):** after annealing	**49**
III.4	Variation in the average thickness before and after annealing of CuO:Cr with different doping levels	**50**
III.5	The optical absorption of CuO:Cr films at different chromium concentrations **(a)** before annealing and **(b)** after annealing	**51**
III.6	Variation of Urbach energy of CuO:Cr thin films before and after annealing	**52**
III.7	Variation of the optical band gap energy of copper oxide thin films doped with chromium before and after annealing	**53**
III.8	Variation of optical band gap and Urbach energy of CuO:Cr thin films at different chromium concentrations **(a)** before annealing and **(b)** after annealing	**54**
III.9	The effect of doping and annealing on the refractive index of CuO: Cr	**55**
III.10	Variation of average film thickness and refractive index of CuO:Cr thin films at different chromium concentrations before annealing **(a)** and after annealing **(b)**	**56**
III.11	Variation of electrical conductivity of CuO: Cr thin films as a function of Cr concentrations before and after annealing	**57**

List of tables

Table No.	Title	Page
I.1	Some properties of Cu_2O	20
I.2	Some optical properties of Cu_2O	20
I.3	Some electrical properties of Cu_2O	21
I.4	Some structural properties of Cu_2O	23
I.5	Some electrical properties of CuO	25
II.1	Some physical properties of $CuCl_2$	34
II.2	Some physical properties of (CrCl3 · 6H2O)	35
II.3	Precipitation conditions for deposition CuO : Cr	36
III.1	Photos of CuO :Cr thin films deposited on glass substrates	47

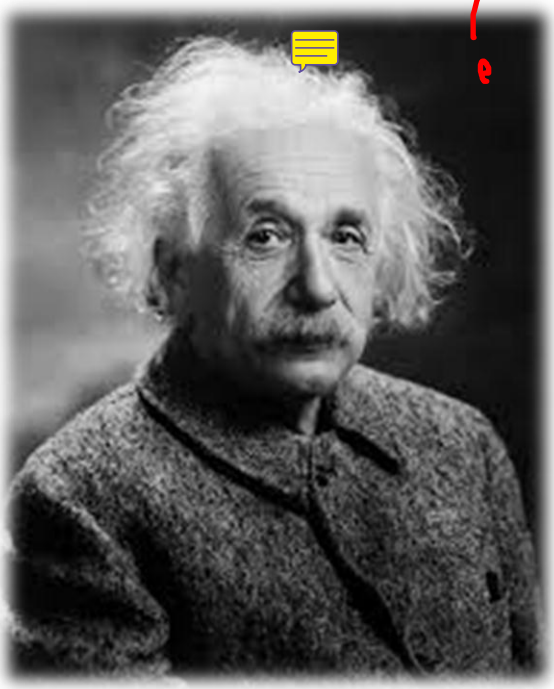
List of symbols

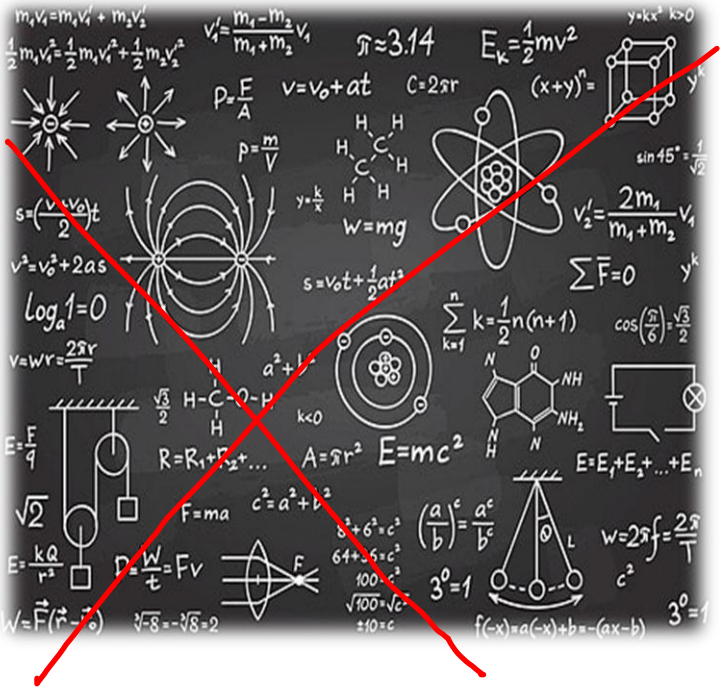
symbol	signification	unit
M	Mass molar	g/mol
C	Solution concentration	mol/l
m	Mass	g
V	Volume	l
Ø	Diameter	m
T	Temperature	^{o}C
α	Absorption coefficient	cm^{-1}
n	Refractiveindex	
K	the proportionality constant	
R	the reflectance	
E_g	Energy of optical band gap	eV
T	Optical transmittance	%
I	Intensity of light	
d	Film thickness	nm
λ	Wavelengthof incident photon	nm
φ_s	Spray flow rate	ml/h
$h\upsilon$	Energy of incident photon	eV
E_{Urb}	Urbach energy	eV
I	Electrical current	A
V	Voltage	V
ρ_s	Surface resistivity	Ω/sqr
σ	Electrical conductivity	$\Omega^{-1}.cm^{-1}$
S	Distance	m

List of abbreviation

CuO	Cupric oxide
Cu_2O	Cuprous oxide
Cu	Copper
Cr	chromium
PVD	Physical vapor deposition
PLD	Pulsed-laser deposition
MBE	Molecularbeamepitaxy
CVD	Chemical vapor deposition
PECVD	Plasma Enhanced Chemical Vapor Deposition
MOCVD	Metal-Organic Chemical Vapor Deposition
UHV-CVD	Ultra-high vacuum chemical vapor deposition
CSD	Chemical solution deposition
Sol – Gel	Solution-gelling
CBD	Chemical bath deposition
TCOs	transparent conducting oxides
FCC	face-centered cubic
LEDs	light-emitting diodes
USP	Ultrasonic Spray Pyrolysis
$CuCl_2.2H_2O$	copper(II) chloride dihydrate
CrCl3 6H2O	chromium(III) chloride hexahydrate
LMSSEF	Laboratoire des matériaux et structure des systéms électromécaniques et leur fiabilité
UV – Vis – NIR	Ultraviolet-visible-near infrared

General introduction





General introduction

General Introduction

Metal oxide semiconductors are highly attractive materials due to their unique properties. they are known for being abundant in nature, environmentally friendly, easy to synthesize, and cost-effective [1]. In recent decades, there has been growing interest in the field of conductive metal oxides, particularly compounds such as copper oxide (CuO and Cu_2O) and chromium oxide (Cr_2O_3). These materials exhibit outstanding performance in various industrial applications, such as photovoltaic cells, laser diodes, gas sensors and others[2,4].

These materials are generally classified as wide bandgap semiconductors and are divided into two main types based on their conduction mechanism: n-type (electron conduction) and p-type (hole conduction). In recent years, p-type metal oxides have attracted considerable research interest, particularly chromium oxides and copper oxides [5,6]. Copper oxide exists in two stable crystalline forms: cupric oxide (CuO) and cuprous oxide (Cu_2O), both of which are p-type semiconductors with wide and direct optical bandgaps of approximately 1.2 eV for CuO and 2.1 eV for Cu_2O [7]. They also exhibit high electrical conductivity. The most stable. Both oxides are being studied as possible candidates for optoelectric and electrochemical applications [8].

Chromium oxide is an inorganic compound that exists in various chemical forms such as CrO and CrO_2, but the most widely recognized and utilized form is Cr_2O_3 [9]. This compound naturally occurs as a rare mineral known as "Eskolaite" and is considered one of the most important chromium oxides due to its distinctive properties. Cr_2O_3 appears as a green-colored substance and is classified as a p-type semiconductor with a direct band gap of 3 eV [10]. It is widely used in several fields, including the manufacture of heat-resistant bricks for furnaces. It is also incorporated into glass and mirrors to reduce light reflection, and employed in magnetic storage media for audio and video recording. Additionally, Cr_2O_3 serves as a polishing agent for fine surface finishing of materials such as gemstones, diamonds, and glass [11].

Several techniques are available for the preparation of undoped and chromium-doped copper oxide thin films, such as chemical deposition, thermal evaporation, and sputtering, in addition to more advanced methods like sol–gel, chemical vapor deposition, and spin coating [12]. However, spray pyrolysis—particularly the ultrasonic variant—is considered one of the most common and effective techniques due to its simplicity, low fabrication cost, and ability to deposit uniform films over large areas at relatively low temperatures [13,14,10].

General introduction

This work aims to develop thin films of undoped and chromium-doped copper oxide (CuO) at various atomic concentrations using the ultrasonic spray pyrolysis technique on glass substrates heated to 350°C. The films were deposited from an aqueous solution of copper(II) chloride dihydrate ($CuCl_2 \cdot 2H_2O$) and chromium(III) chloride hexahydrate ($CrCl_3 \cdot 6H_2O$), with a fixed distance between the nozzle and the substrate.

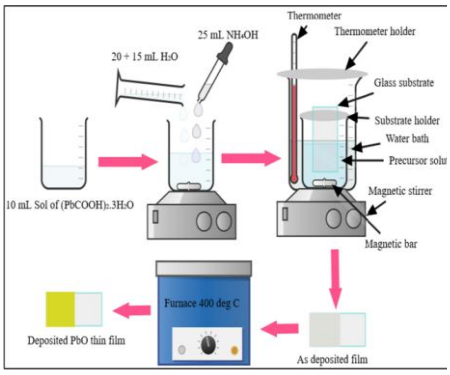
The study focuses on investigating the effect of chromium doping and annealing on the optical and electrical properties of the prepared CuO thin films, while attempting to interpret the observed variations in these properties through changes in the structural and morphological characteristics resulting from doping and thermal treatment.

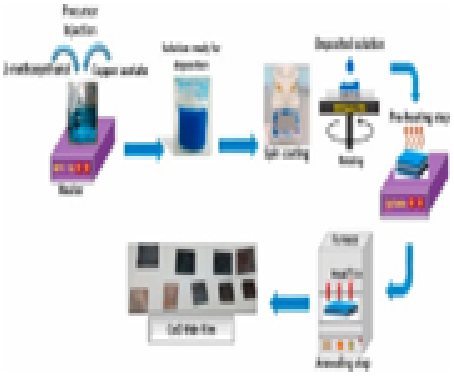
This work was carried out at the Laboratory of Materials and Structure of Electromechanical Systems and their Reliability (LMSSEF) at Larbi Ben M'hidi University in Oum El Bouaghi. The samples were characterized using various techniques, including UV-Vis-NIR spectroscopy and the four-point probe method, in order to accurately determine their optical and electrical properties.

In our thesis, the adopted approach to presenting our work is organized into three chapters:

- The first chapter is dedicated to the concepts of thin films, their preparation techniques, transparent conductive oxides, the fundamental properties of copper oxide, and its fields of application.
- The second chapter focuses on the preparation of undoped copper oxide films and chromium-doped copper oxide films Characterization techniques of thin films.
- The final chapter presents the experimental results obtained (optical and electrical properties) of our samples and discusses the variations in these properties due to the effects of doping and annealing, as well as the relationship between these variations.

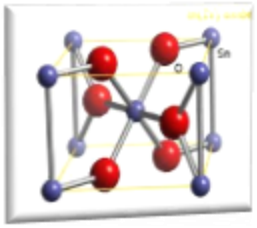
In conclusion, we summarize at the end of this work the general findings that highlight the different stages and the results that have been achieved.





Chapter I

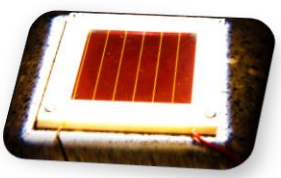
Overview on copper oxide thin film











Chapter I: Overview on copper oxide thin film

In recent years, thin films of metal oxides have become outstanding materials due to their diverse industrial applications[15]. Copper oxide is one of the most prominent among these oxides. This chapter focuses on a bibliographical study of thin films and their deposition methods, reviewing various deposition processes and the general properties of copper oxide, including its structural, optical, and electrical characteristics, as well as its wide range of applications.

I.1. Overview on thin film

Thin film technology is the basic of astounding development in solid state electronics [16], where its studies have directly or indirectly advanced many new areas of research in solid state physics and chemistry which are based on phenomena uniquely characteristic of the thickness, geometry, and structure of the film; they are especially appropriate for applications in microelectronics and integrated optics [16,17].

Thin film is a layer of material ranging from fractions of a nanometer (monolayer) to several micrometers in thickness. This small distance between the two surfaces limits (almost two-dimensional) causes a perturbation of the majority of physical properties [17].

The atoms of thin film grow on a substrate surface arranged predictably in their almost correct crystallographic position [17].

The thin film of the same material and the same thickness may have different physical properties depending on whether it is placed on an amorphous insulting substrate such as glass [18].

I.2. Thin film deposition techniques

Deposition techniques have significantly evolved in our time, leading to the emergence of a wide range of methods that vary based on their applications. The figure I.1 illustrates the most commonly used global methods for preparing thin films. These methods are categorized into two main types :

- Physical methods
- Chemical methods

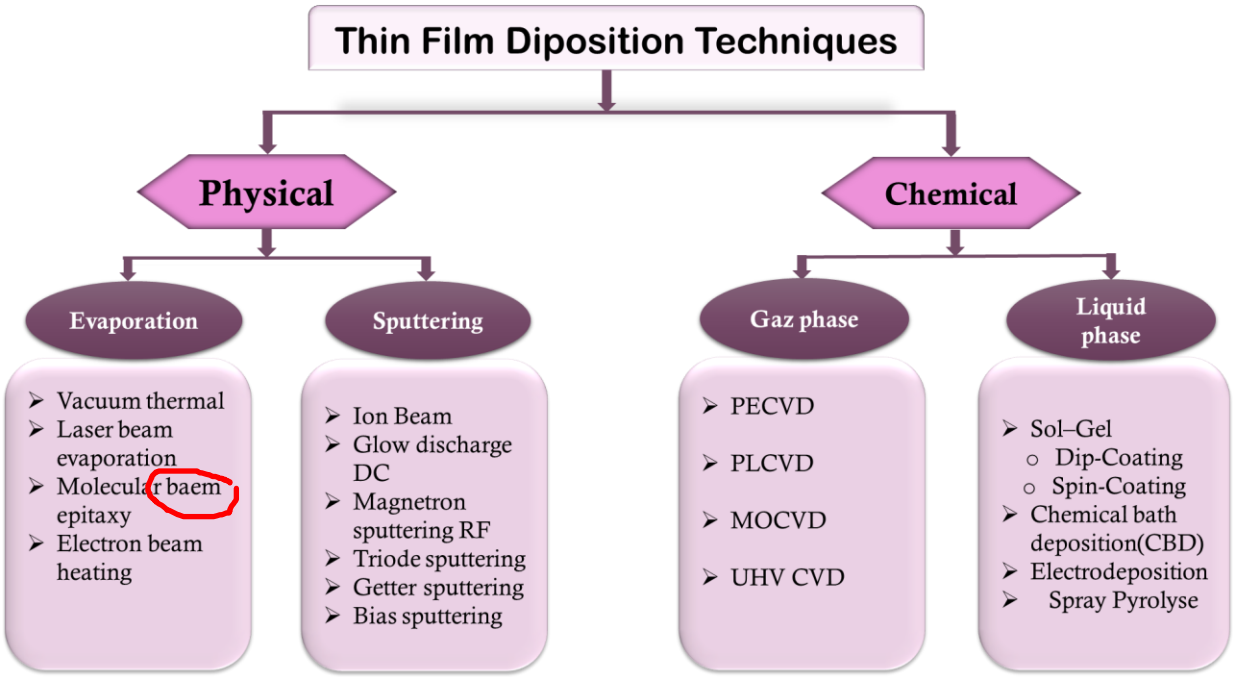


Figure I.1. Thin film deposition techniques.

I.2.1. Physical deposition Methods

Physical methods particularly or Physical vapor deposition (PVD) rely on the freezing or direct ejection of materials from targets while in their gaseous state. The fundamental techniques of this method include evaporation and sputtering in all its forms. These deposition techniques enable the production of a wide range of materials at a relatively low deposition temperature (< 500°C), for example [19].

- Etallic films (such as Al, Cu, Ti, etc.) and their alloys
- Refractory metal films (such as Mo, Ta, W, etc.).
- Oxide films (such as ZrO_2, SiO_2, Al_2O_3, TiO_2, etc.).
- Films of nitrides, silicides, carbides, borides, and fluorides.

Physical methods offer many advantages over chemical methods, such as producing dense films, ease of process control, and the absence of pollution [20].

I.2.1.1. Stages of formation of thin films by physical methods

The following main stages often occur in the physical methods : nucleation (atom deposition), coalescence, and growth.

➢ Particle nucleation stage

This stage corresponds to the changes that occur at the material state level and represents the moment when the material transitions into a new state, whether chemically or physically.

These materials are transformed into a nucleus and deposited on the substrate surface. They are formed thermally by the interaction of the material's atoms with the substrate surface, leading to the formation of what is known as agglomerates, as illustrated in figure I.2 [21].

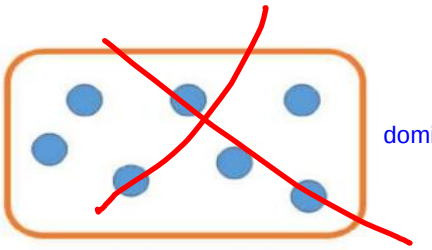
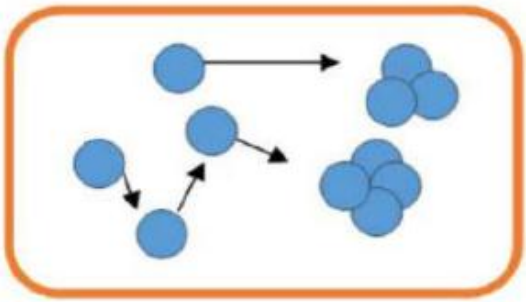


Figure I.2. A schematic diagram illustrating the nucleation stage of thin film deposition [15].

➢ The coalescence stage

It'is the second step in the formation of a thin film, where stable island growth occurs by increasing the size of the nuclei formed in the previous stage and merging them together (Figure I.3). Coalescence can be accelerated by increasing the mobility of condensed materials on the surface (e.g., by increasing the substrate temperature). When these islands reach a certain density, they flatten to increase coverage and merge with each other. If the probability that all islands on the substrate are oriented in the same direction is low, this coalescence results in a polycrystalline structure. In the opposite case, a single-crystal thin film is formed [22,23].

As a result, achieving a single-crystal thin film is not always possible.



where is surface change this image

Figure I.3. A schematic illustrating the coalescence stage [15].

➢ The growth stage

It'is the final step in forming a thin film. This phenomenon is considered a continuation of the bonding process, where a continuous layer forms on the substrate surface by filling the gaps (voids). The boundaries between the formed nuclei are called grain boundaries, as shown in Figure I.4 [24].

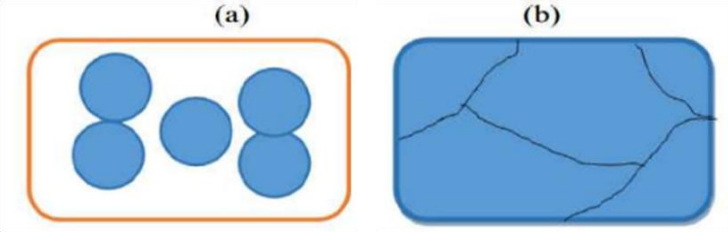


Figure I.4. A diagram illustrating the stages of coalescence and growth of thin fims [15].

The growth modes were classified by Ernst Bauer in 1958 into three modes (Figure I.5) [25] :

- Layer Growth (Frank–Vander Merwe): This mode of growth is two-dimensional (2D), where atoms are deposited layer by layer on the substrate surface. This mode of growth occurs when the interaction between the deposited atoms is stronger than their interaction with the substrate, leading to the formation of thin and continuous layers.
- Island Growth (Weber–Volmer): This mode of growth is three-dimensional (3D), where the growth process occurs in the form of isolated islands on the surface.
- Layer-Plus-Island Growth (Stranski–Krastanov):This is an intermediate growth mode between the first two modes. Initially, the growth starts as a 2D layer, but after depositing a certain number of layers, the surface energy leads to the formation of 3D islands.

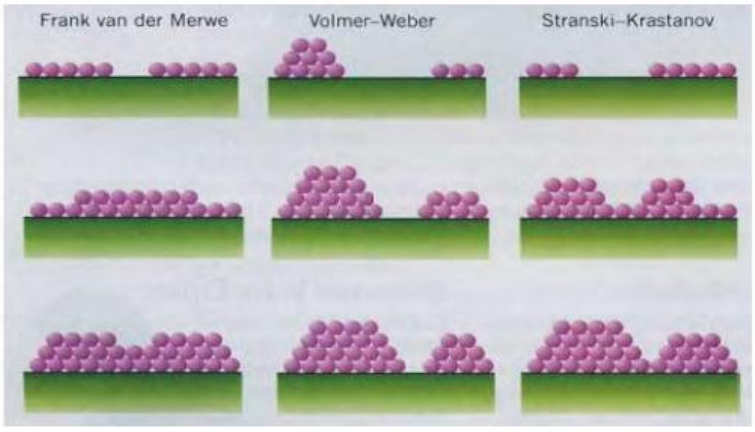


Figure I.5. Growth modes of thin films [26].

I.2.1.2. Vacuum evaporation techniques

In this technique, the interconversion between the solid and vapor phase takes place in a vacuum environment. There are several evaporation methods available for thin-film deposition [27].

A. Thermal evaporation technique

This technique relies on heating the material to high temperatures until evaporate. The process takes place inside a vacuum chamber with an air pressure ranging between 10^{-4} Pa and 10^{-3} Pa [28].

Condensation and deposition occur on the surface of the substrate when this substance evaporates, forming a thin layer. The speed of deposition of these substances depends on two main factors: the distance between the evaporating substance and the substrate and the temperature of the source[15].

The surface of substrate must be vertically aligned with the vapor flow to achieve optimal results [29]. The figure I.6 illustrates vacuum deposition machine and its principle [30].

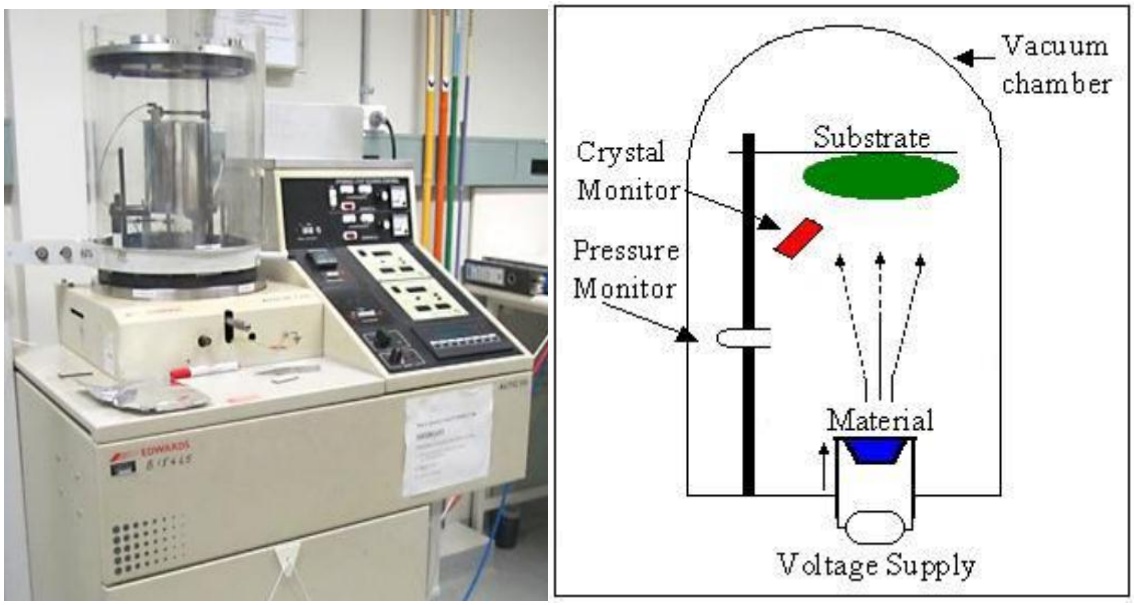


Figure I.6. Thermal evaporation technique machine and its diagram [31].

B. Laser beam evaporation (Laser ablation)

Laser ablation is the process of removing material from a solid surface by irradiating it with a laser beam. At low laser flux, the material is heated by the absorbed laser energy and evaporates or sublimates. At high laser flux, the material is typically converted to plasma. Usually, laser ablation refers to removing material with a pulsed laser (Figure I.7), but it is possible to ablate material with a continuous wave laser beam if the laser intensity is high enough. In general, the method of pulsed laser deposition (PLD) is simple. Only few parameters need to be controlled during the process. Targets used in PLD are small compared with other targets used in other sputtering techniques. It is quite easy to produce multi-layer film composed of two or more materials. Besides, by controlling the number of pulses, a fine control of film thickness can be achieved [32].

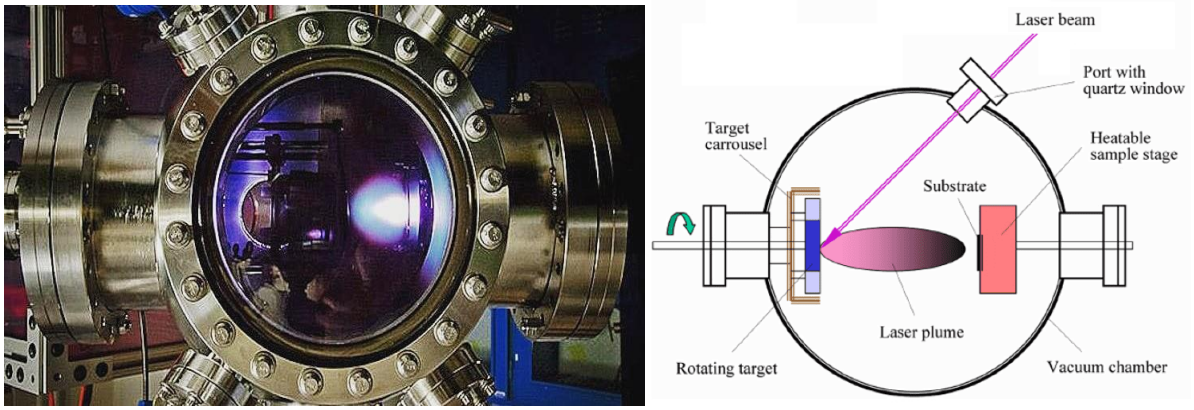


Figure I.7. Pulsed laser deposition machine and its diagram [33].

C. Molecular beam epitaxy (MBE)

This technique is based on the sublimation by heating of the elements to be deposited and their condensation on the surface of a substrate, without interaction between the precursors other than on the substrate (figure I.8). Although this method is suitable for depositing monocrystalline films in epitaxy relationship with the substrate with excellent control of the thickness, it presents the disadvantages of imposing a very high vacuum (10^{-12} bar) and of being very slow (about one single layer per second). The films deposited are very sensitive to the quality of the substrate [34].

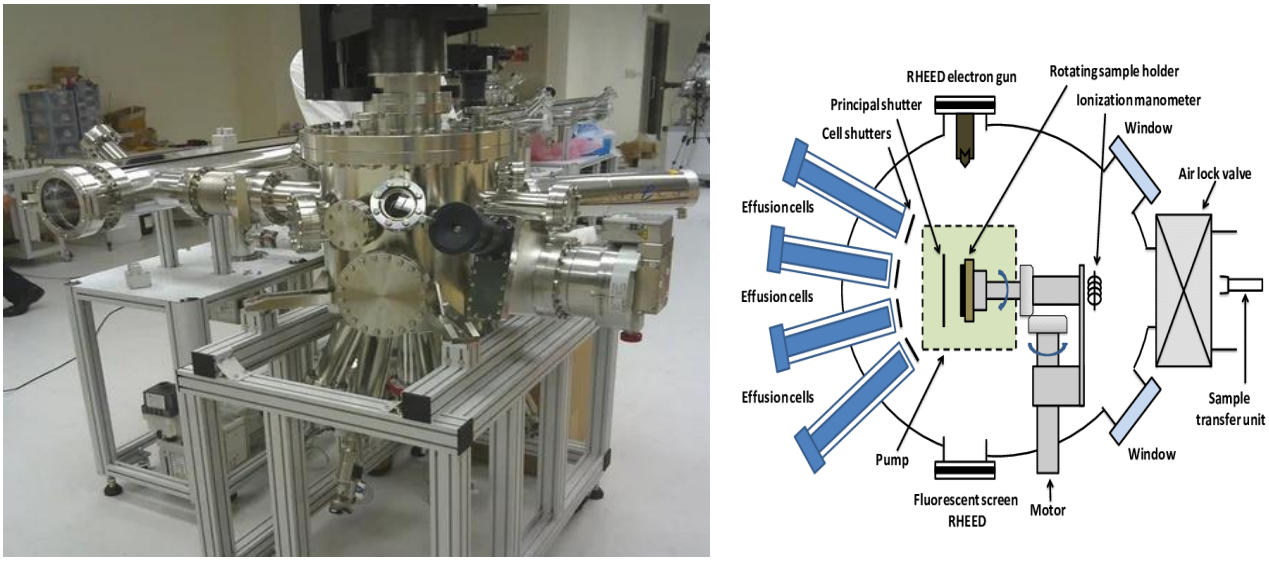


Figure I.8. Molecular beam epitaxy (MBE) machine and its diagram[17].

D. Electron beam heating

The principle of this method is presented in Figure I.9. The electron beam generated by a tungsten filament (W) is deflected by an electromagnet towards the crucible containing the material. This technique has two important advantages [17,35,36]:

- It is easy to control the applied power, therefore the evaporation rate. Consequently, the deposition on the substrates can be easily controlled in a wide range of speeds, from very low to very high.
- The material to be evaporated is placed in a water-cooled copper crucible, which eliminates the problems due to contaminations by the crucible.

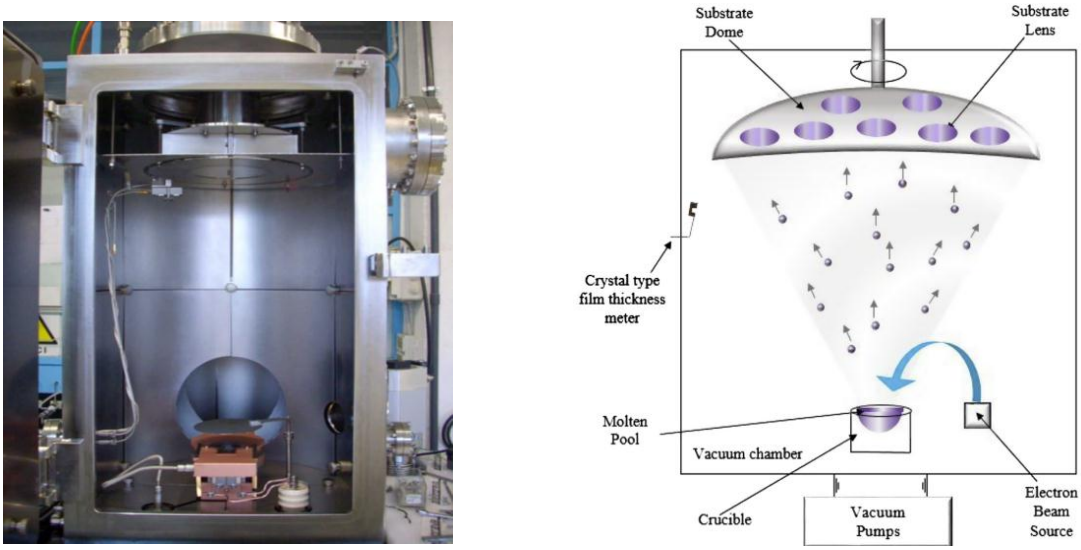


Figure I.9. Electron beam heating machine and its diagram[37].

1.2.1.3. Sputtering technique

Sputtering technique is mostly used for depositing films by controlling the crystalline structure and surface roughness. The simple form of the sputtering system consists of an evacuated chamber containing metallic anode and cathode in order to obtain a glow discharge in the residual gas in the chamber. Also, an applied voltage in the order of several KeV with pressure more than 0.01 mbar is sufficient for film deposition. The sputtering process depends on the bombardment of the ions released from the discharge to the molecules in the cathode leading to the liberation of the molecules from the cathode with higher kinetic energy . The atomic weight of the bombarding ions should be nearly to that of the target material in order to maximize the momentum transfer. These molecules move in straight lines and strike on the anode or on the substrate to form a dense thin film. The diagram of the sputtering system is shown in Figure I.10 [38].

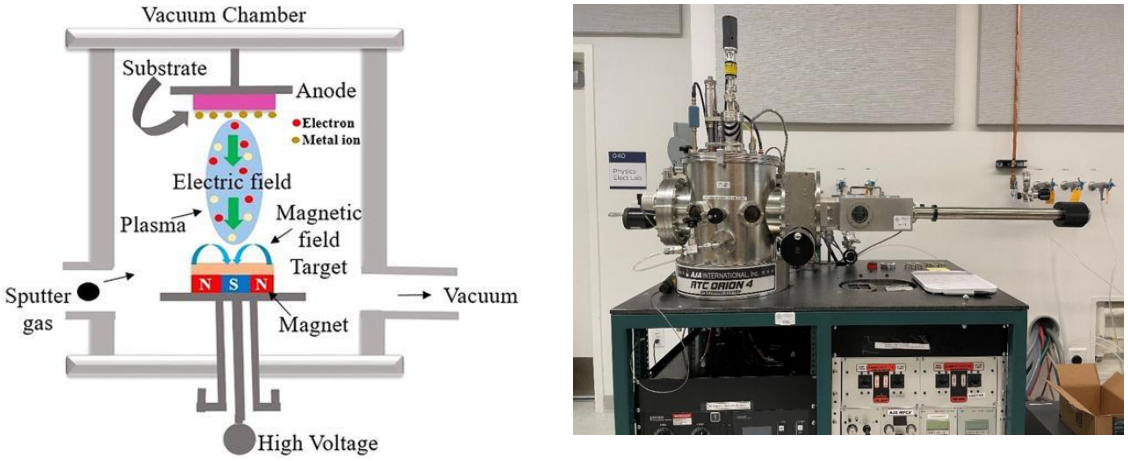


Figure I.10. Sputtering technique machine and its diagram [37].

I.2.2. Chemical deposition Methods

Chemical methods also primarily depend on chemical reactions that result in material formation. When classifying these methods, they can be divided into two main categories: the first involves film formation chemically from components added to the medium, while the second refers to film formation through chemical reactions between intermediate components.

I.2.2.1. Chemical vapor deposition (CVD)

Chemical Vapor Deposition (CVD) is an advanced industrial technique used to deposit thin solid layers on substrate surfaces by chemically reacting gas-phase constituents at or near

the surface to form a solid product. This method is among the most efficient and precise for thin film formation, especially in applications that require strict control over thickness and structural composition [39].

The CVD process involves a sequence of integrated steps: introducing reactive gases into the reaction chamber, activating these gases using heat or plasma to initiate chemical reactions, followed by adsorption of the active gases on the substrate surface. The chemical reactions then occur on the surface, forming the solid film. Volatile byproducts are subsequently transported away, and waste gases are exhausted [39].

This technique encompasses several scientific disciplines, including gas-phase chemistry, thermodynamics, kinetics, transport mechanisms, and reactor engineering. The fundamental chemical reactions involved include pyrolysis, oxidation, reduction, hydrolysis, nitride and carbide formation, synthesis reactions, disproportionation, and chemical transport [39].

Several factors influence the deposition rate and the quality of the resulting film, such as temperature, pressure, input concentrations, gas flow rates, reactor geometry, and the operating principle. Together, these parameters allow for precise control over film characteristics, making CVD a key technology in many industrial applications, particularly for coating substrates under low pressure and at high temperatures [39].

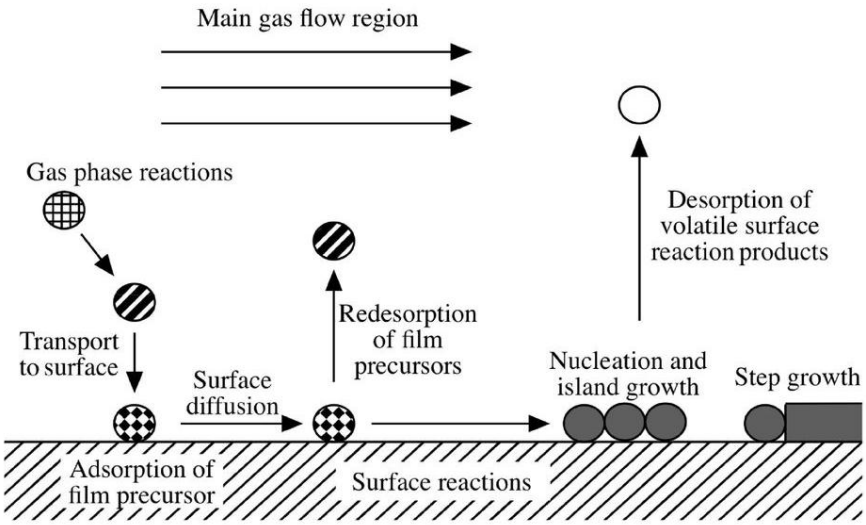


Figure I.11. CVD steps thin film formation [40].

A. Plasma enhanced chemical vapor deposition (PECVD)

PECVD is a plasma-enhanced CVD process where deposition is achieved by introducing reactant gases between a grounded electrode and an energized electrode (Figure I.12). The capacitive coupling between the electrodes excites the reactant gases into plasma, which induces a chemical reaction and results in the reaction product being, deposited on the substrate. The gear, which is placed on the grounded electrode, is typically heated to 300°C. PECVD is used to deposit thin films of various materials on substrates at lower temperature than that of standard CVD technique [41].

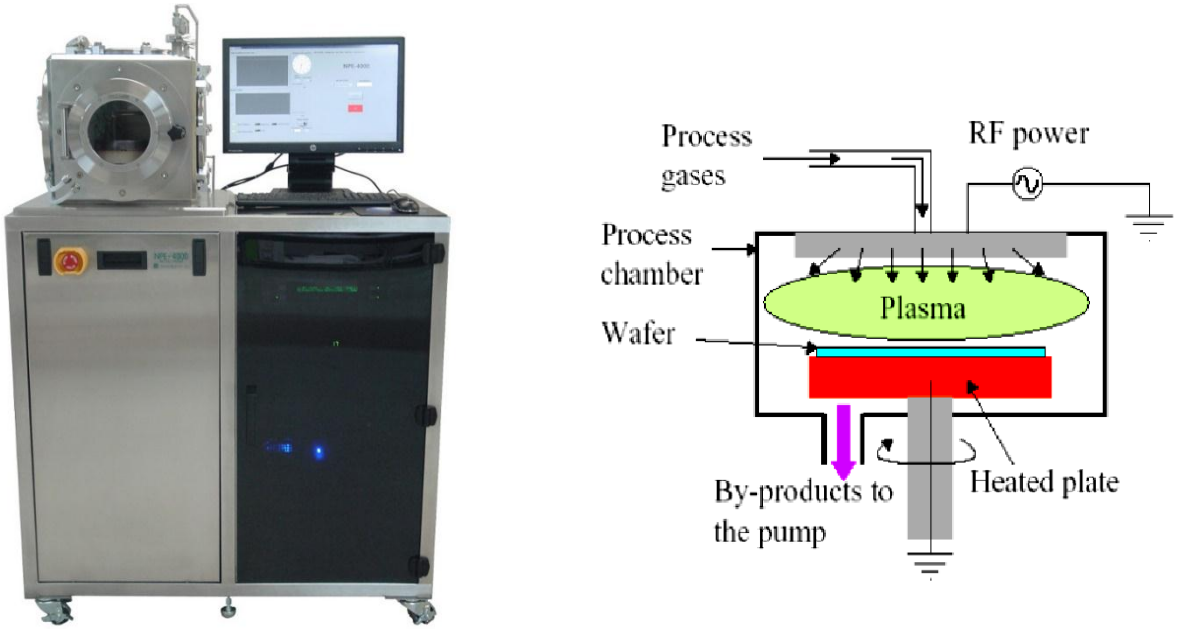


Figure I.12iagram and machine PECVD[17].

A. Metal-organic chemical vapor deposition (MOCVD)

MOCVD (Metal-Organic Chemical Vapor Deposition), at atmospheric or low pressure, is a technique inherited from microelectronics, where many surface depositions are performed using CVD (Chemical Vapor Deposition), such as polysilicon or silica at low temperatures. This process involves bringing a volatile compound of the material to be deposited into contact with the substrate [35].

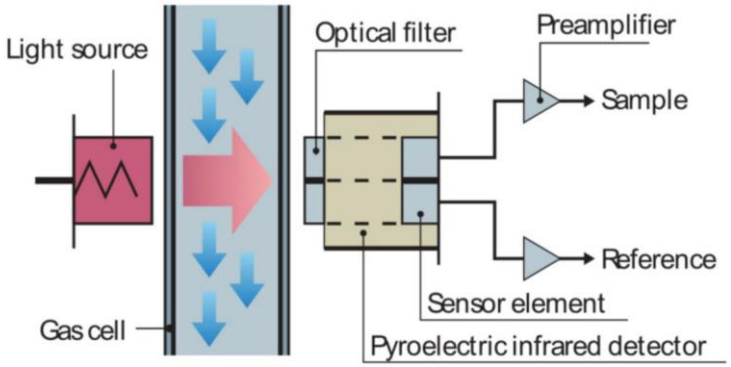


Figure I.13. MOCVD system diagram [35].

B. Ultra-high vacuum chemical vapor deposition (UHV-CVD)

In this method (Figure I.14), thin films are deposited under a pressure lower than 10 Pa to minimize contamination of the thin films by gases present in the experimental environment [15].

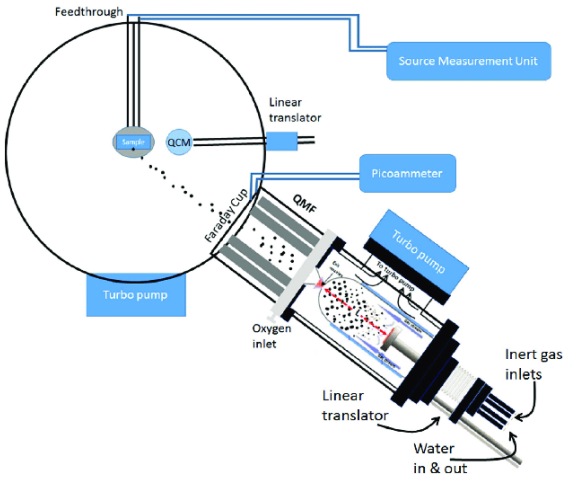


Figure I.14. UHV-CVD system diagram[15]

I.2.2.2. Chemical solution deposition (CSD)

A. Sol–Gel technique

• **Sol:** a stable suspension of colloidal solid particles or polymers in a liquid.

• **Gel:**porous, three-dimensional, continuous solid network surrounding a continuous liquid phase.

Sol-gel is a chemical synthesis technique for preparing glasses, gels and ceramic powders. For the purposes of many theses, it will serve as an easy way to make high purity glass in solution

form at room temperature. In the sol-gel process, a system of colloidal particles in a solution (sol) becomes a macroscopic material (gel), which is interpenetrated by a liquid [42].

There are two main sol-gel methods :

- **Dip-Coating method:** is used less frequently. It involves immersing the substrate in the solution to be deposited and then withdrawing it at a constant rate, which affects the thickness of the deposited layer [43].

After the deposition process, the layer is dried and then heated to achieve crystallization.

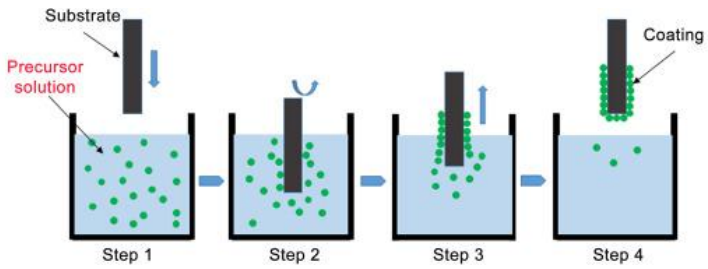


Figure I.15. dip coating basic process [44].

- **Spin-Coating or centrifugation method** : involves pouring the sol or gel onto the surface of a substrate that rotates at a specific speed. The centrifugal force causes the liquid to be expelled, while the thickness of the deposited layer depends on the rotation speed of the substrate and the deposition time [43].

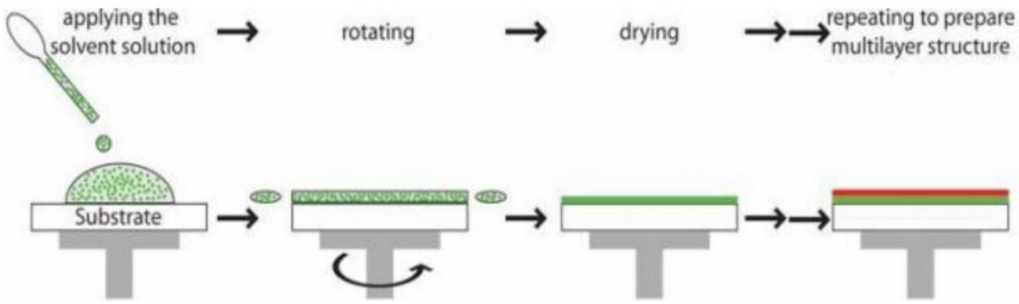


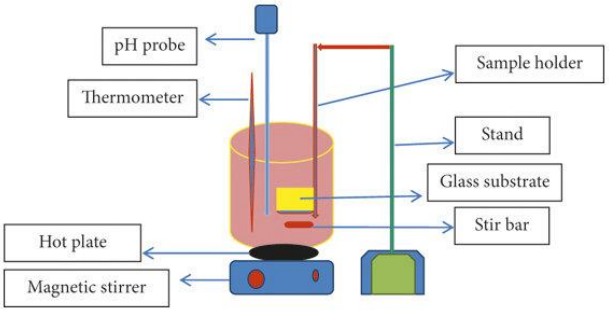
Figure I.16. Spin-Coating basic process[45].

B. Chemical bath deposition technique

Chemical bath deposition (CBD) is also known as solution growth technique or controlled precipitations. It is the oldest method to deposit films on a substrate [46] . The deposition can

be performed at lower temperatures. It is based on the formation of a solid phase from a solution.

In the chemical bath deposition procedure, the substrate is immersed in a solution containing the precursor. This method depends upon parameters such as bath temperature, pH of the solution, the molarity, and time. Figure I.17 represents the simple chemical bath deposition method[46].



FigureI.17. Chemical bath deposition technique [47].

C. Electrodeposition

An electric current is passed through an electrolytic solution containing metal ions to be deposited between a metallic electrode and the substrate. The deposition will only occur on the parts of the substrate covered with this initial metallic layer, as shown in Figure I.18. The thicknesses range of film obtained by using this technique from a few micrometers to several hundred micrometers [48].

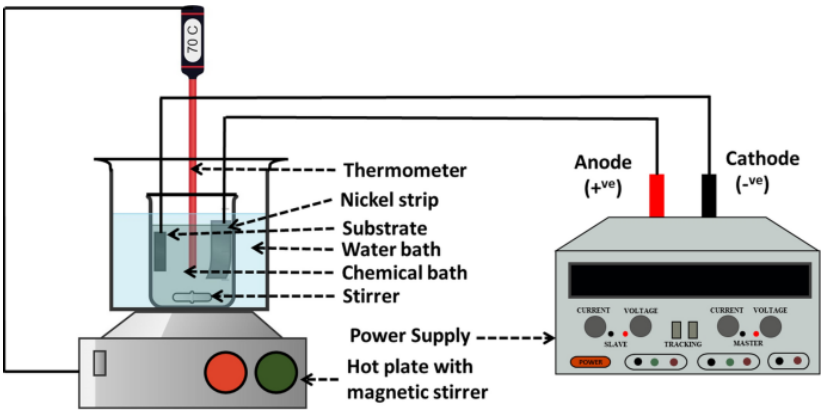


Figure I.18. Electrodeposition diagram [49].

D. Spray pyrolyse

This technique relies on dissolving the source material to be deposited in a suitable solution (precursor solution) and then spraying it in the form of fine droplets. These droplets (containing tens of microns per drop) are sprayed onto a hot substrate at an appropriate temperature. A chemical reaction occurs between the heated surface and the liquid droplets, resulting in the deposition of a thin film of the desired material[50].

This technique was first used by Hottel and Unger in 1959, where they successfully deposited a NiO film on an aluminum substrate[51].

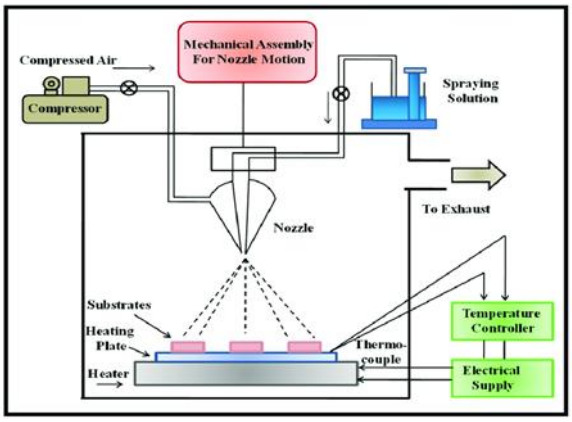


Figure I.19. Pyrolysis Spraying diagram [52].

I.3. Transparent conductive oxides

I.3.1. Definition

Transparent conductive oxides (TCOs) are binary or triple compounds, which contain one or more of the metallic elements, consisting the metal atoms and atoms of oxygen ($M1_xM2_yO_z$), where M is the chemical symbol of the Metal atom considered, O the symbol of the oxygen atom, “x” and “y” and “z” natural whole numbers , for examples:

•Aluminum oxide: Al_2O_3.

•Zinc oxide: ZnO.

•Copper oxide: CuO.

•Iron oxide: Fe_2O_3.

•Tin oxide: SnO_2.

Conductive transparent oxides forma class of materials combining two properties: electrical.

conduction and transmittance in the visible range of light . TCOs are used in several areas of application. So, Therefore, they are found in drones' aircraft, satellite networks, flat screens , anti-freeze windows, heat-reflecting windows (Buildings, ovens, etc.), electromagnetic shields, electrostatic charge dissipators, photovoltaic cells and modules [53].

I.3.2. Metal oxides

Metal oxides are important materials widely used as solid catalysts. They are classified as heterogeneous catalysts and are applied in acid-base and redox reactions. Transition metals, in particular, have attracted significant attention due to their unique electronic configuration [54]. Metal oxides are formed when metals, which act as cations, react with oxygen. These compounds consist of at least two elements, always including oxygen, whether in a single atom or more. They tend to be solid, basic, and denser compared to non-metallic oxides. The oxygen ions in these oxides carry a negative charge [55]. These oxides are widely used in various chemical reactions, including oxidation, dehydration, dehydrogenation, and isomerization. Certain transition metal oxides, such as Nb_2O_5, WO_3, and TiO_2, are commonly employed as heterogeneous acidic nanocatalysts. These oxides feature mesoporous structures that allow reactant molecules to enter the metal pores, facilitating the catalytic reaction [56]. Metal oxides are categorized into two main types:

1. p-type oxides: These conduct via holes and are relatively unstable due to their tendency to lose or exchange oxygen with the air [17].

2. n-type oxides: These conduct via electrons and are more stable, making them the preferred choice for gas sensor applications [17].

I.4. Copper oxide: properties and applications

I.4.1.Formation of copper-based oxides

Copper is a chemical element with the symbol "Cu". When it reacts with oxygen (i.e., when it oxidizes), it forms two thermodynamically stable oxides. That means these oxides do not easily break down or change at normal temperatures. The two stable types are [57,58] :

- Cuprous oxide (Cu_2O), also known as cuprite

- Cupric oxide (CuO), also known as tenorite

These oxides are formed through the following chemical reactions [8]:

$$4\,Cu + O_2 \Leftrightarrow 2\,Cu_2O \quad \text{(I.1)}$$

$$2\,Cu + O_2 \Leftrightarrow 2\,CuO \quad \text{(I.2)}$$

$$2\,Cu_2O + O_2 \Leftrightarrow 4\,CuO \quad \text{(I.3)}$$

CuO can be formed either directly from metallic copper during its transition from the metallic state to the oxide state **(Eq. I.2),** or from Cu_2O through a phase transformation

(Eq. I.3). This process depends on several factors such as the partial pressure of oxygen, temperature, and oxidation duration[8].

There is also a transitional phase between cuprite (Cu_2O) and tenorite (CuO), known as Cu_4O_3. This compound has an energy potential very close to that of Cu_2O and CuO. However, according to the literature, this phase is not thermodynamically stable[5 ,59].

Copper oxides, CuO and Cu_2O, exhibit a range of remarkable properties that can be fully utilized in various fields. They are particularly explored for potential applications in solar cells, catalysis, superconducting materials, magnetic storage devices, gas sensors, as well as photothermal and photoconductive systems. At the nanoscale, changes in their electronic structure significantly affect their properties due to quantum confinement effects[60].

I.4.2. Cuprous oxide (Cu_2O)

- **I.4.2.1. Crystallographic structure**

Cuprous oxide (Cu_2O) is a red-brown compound, as shown in Figures I.20 (a and b). While it can be synthesized most commonly by oxidizing metallic copper (Eq. I.1), this method is typically used when the goal is to produce it in bulk form rather than as thin films. Cu_2O also occurs naturally as a mineral known as cuprite.



Figure I.20. Cuprous oxide "Cu_2O"; (a): in the form of natural cuprite, and (b): powder

Cuprous oxide (Cu_2O) is a stable phase in the binary copper-oxygen system, and it crystallizes in a cubic structure. Its unit cell consists of six atoms: four copper atoms arranged in a face-centered cubic (FCC) lattice at the (1/4, 1/4, 1/4) positions, and two oxygen atom located at the tetrahedral sites at (3/4, 3/4, 3/4), as illustrated in Figure I.21. In this arrangement, each copper atom is coordinated with two oxygen atoms as its nearest neighbors, while each oxygen atom is coordinated with four copper atoms. This unique atomic configuration results in distinct interatomic distances between Cu–O, Cu–Cu, and O–O[60,61,62].

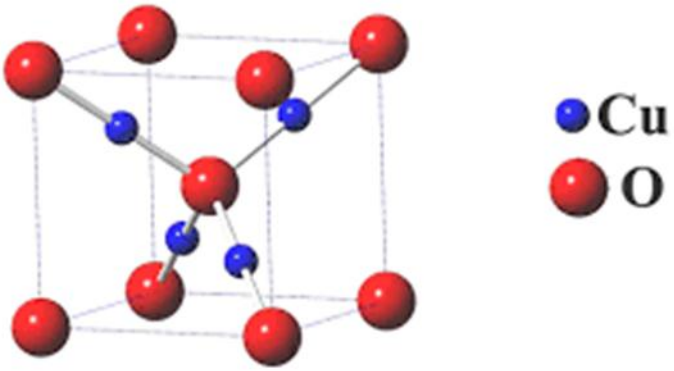


Figure I.21. Crystallographic structure of Cu_2O [63].

Table I.1 represents some properties of Cu_2O

Table 1.1. Some properties of Cu_2O [64,5].

Chemical name	Copper(I) oxide Cuprous oxide
Mineral form	Cuprite
Appearance	Red-brown powder
Solubility in water	Insoluble
Melting point (°C)	1235
Boiling point (°C)	1800
Space group	Pn3m
lattice Mesh parameter (Å)	4.2696
Volume of a cell ($Å^3$)	77.83
Molar volume ($cm^3.mol^{-1}$)	33.44
Density ($g.cm^{-3}$)	6.106
Coordination "Z"	2
Cu–O bond length (Å)	1.85
Cu–Cu bond length (Å)	3.02
O–O bond length (Å)	3.68

- **I.4.2.2. Optical properties**

Copper oxide Cu_2O is known as absorbing material in the visible and near-infrared regions. They exhibit an optical band gap that can vary over a wide range and show high absorption levels (Table I.2) [64,65].

Table I.2. Some optical properties of Cu_2O [64].

Transmittance in the visible range (%)	40
Refractive index	2.24
Absorption coefficient (cm^{-1})	0.12
Optical band gap (eV)	1.8

- **I.4.2.3. Electrical properties of Cu_2O**

The properties of cuprite, particularly its electrical characteristics, have been extensively studied. This oxide, whether in bulk or thin-film form, is a p-type semiconductor exhibiting high mobility of positive charge carriers at room temperature, with a hole mobility around $\mu p \approx 100\ cm^2 \cdot V^{-1} \cdot s^{-1}$ in thin-film form. This mode of conduction is mainly attributed to the presence of copper vacancies at room temperature. Thus, this oxide can be represented as $Cu_{2-y}O$ [5].

Table I.3 shows the variation of electrical conductivity according to different fabrication techniques.

Table I.3. Some electrical properties of Cu_2O [8].

Effective mass of the electron in the conduction band	0.98 m_e
Effective mass of the hole in the valence band	0.58 m_e
Relative dielectric constant	7.5
Thermal conductivity (W K^{-1} m^{-1})	4.5
Nature of the forbidden band	Direct
Type of conductivity	P
Electrical conductivity ($(\Omega.cm)^{-1}$)	10^{-8}-10^{-2}
Concentration of intrinsic carriers (cm^{-3})	10^{13}-10^{18}

Band gap type

I.4.2. cupric oxide (CuO)

I.4.2.1.Crystallographic structure

Copper (II) oxide is a solid semiconductor material of the p-type. It consists of basic metal oxides and exists in the form of a brownish-black powder with a dark brown color. It is odorless and non-toxic, making it easy to obtain and cost-effective to produce[66].

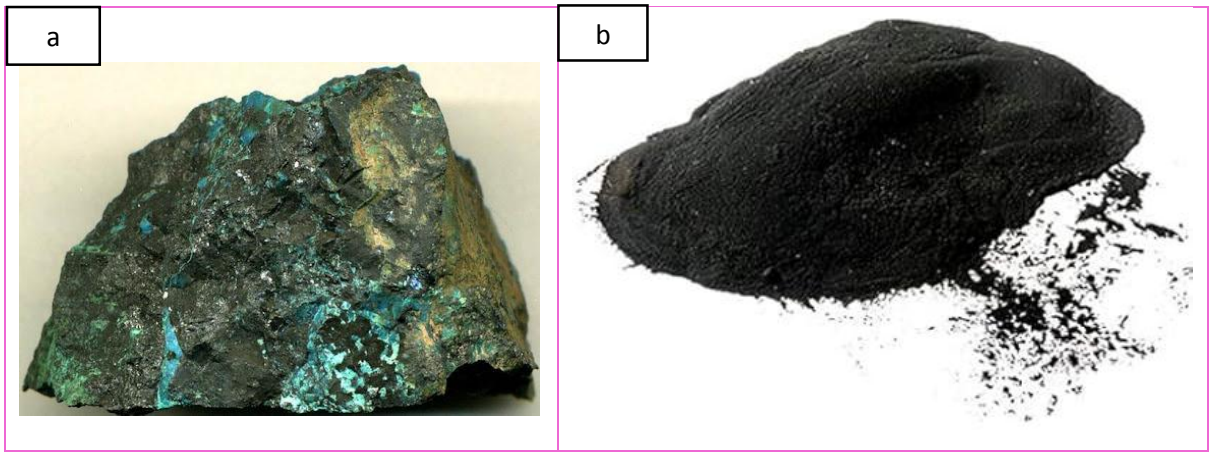


Figure I.22. Copper oxide "CuO" in the form of natural tenorite **(a)** and powder **(b)**.

Copper oxide has a monoclinic crystal structure of the base-centered cubic (BCC) type, where each unit cell contains four CuO units. Each Cu or O atom is surrounded by four neighboring atoms of the opposite type, with a unit cell occupancy of Z = 4 [63].

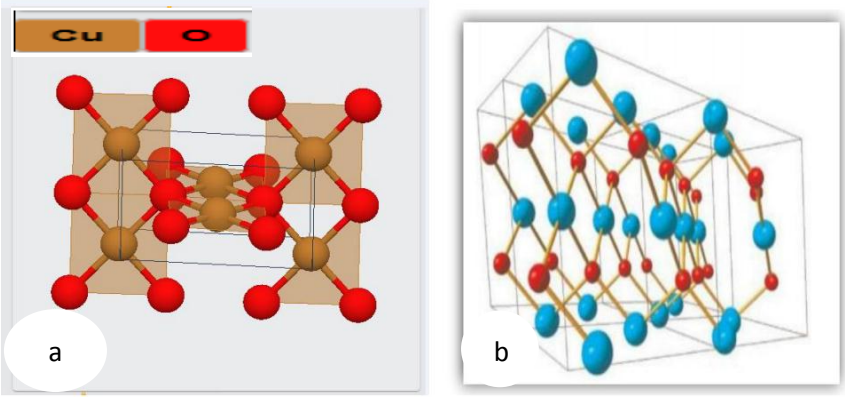


Figure I.23. Structure cristalline de CuO **(a)** une cellule unitaire **(b)** quatre cellules unitaires [67,68].

Table I.4. Some structural properties of Cu_2O [69,64,5].

Chemical formula	Copper (II) Oxide
Mineral form	Tenorite
Appearance	Black powder
Solubility in water	Insoluble
Molar mass(g/mol)	79.545
Boiling point (°C)	2000
Melting point (°C)	1134
Space group	C2/e
Mesh parameter (Å) lattice parameters	a= 4.6837 b=3.4226 c=5.1288 α=β=90° γ=99.548°
Volume of a cell ($Å^3$)	81.08
Atomic radius (Å)	0.69
Density ($g/cm^{3)}$	6.31
Cu–O bond length (Å)	1.96
Cu–Cu bond length (Å)	2.62
O–O bond length (Å)	2.90

I.4.2.2. Optical properties of copper (II) oxide

Copper(II) oxide (CuO) is a p-type semiconductor with an indirect band gap ranging from 1.2 to 1.9 eV (Figure I.24), which enables strong absorption in the visible and near-infrared regions (Figure I.25) [69]. Its optical properties are influenced by intrinsic effects, such as transitions between the valence and conduction bands including excitonic interactions, as well as extrinsic effects due to impurities or defects that introduce energy states within the band gap [19].

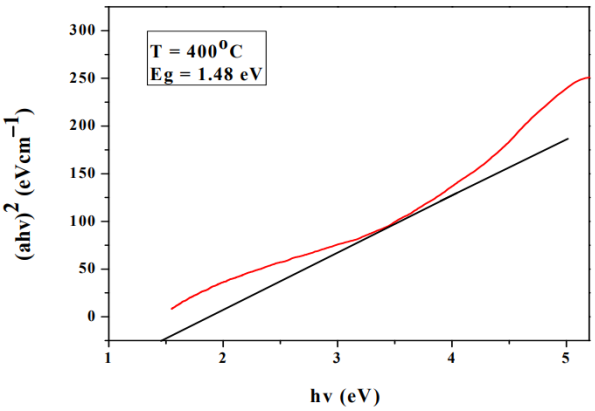


Figure I.24. The Bandgap of CuO thin film[70].

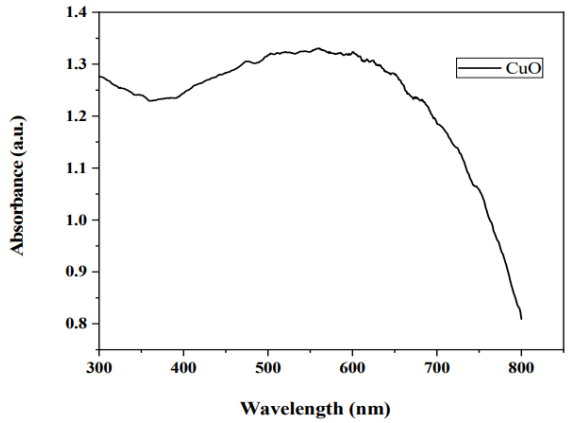


Figure I.25. The UV-visible absorption spectra of CuO thin film[70].

CuO thin films strongly absorb across the visible spectrum, giving them a black appearance [71]. The absorption coefficient ranges between 10^4 and 10^5 cm^{-1} in the visible range, reaching 10^4 cm^{-1} at 500 nm, with a cutoff wavelength around 680 nm [69]. The refractive index varies from 1.5 to 3.5 depending on the deposition method [72,73], while the transmittance can range from 0% to 80% based on deposition temperature, thermal treatment, and doping level [69]. In some cases, it can reach up to 90% at higher visible wavelengths [74]. Films prepared by spray pyrolysis using hydrated copper chloride ($CuCl_2 \cdot 2H_2O$) at different molarities have shown promising optical behavior for solar photothermal applications, with high absorption ($\alpha \geq 0.90$) and low emissivity ($\varepsilon \leq 0.2$) [5].

I.4.2.3. Electrical properties of CuO

The electronic structures of oxygen and copper are [64] :

$Cu^{29} : 1s^2\ 2s^2\ 2p^6\ 3s^2\ 3p^6\ 3d^{10}\ 4s^1$ redundancy

$Cu^{29} : [Ar]_{18}\ 3d^{10}\ 4s^1$

$O^8 : 1s^2\ 2s^2\ 2p^4$

The 2p states of oxygen form the valence band and the 4s states of copper constitute the conduction region of the copper oxide semiconductor. Table I.5 lists some electrical properties of CuO.

Tableau I.5. Some electrical properties of CuO [5,64].

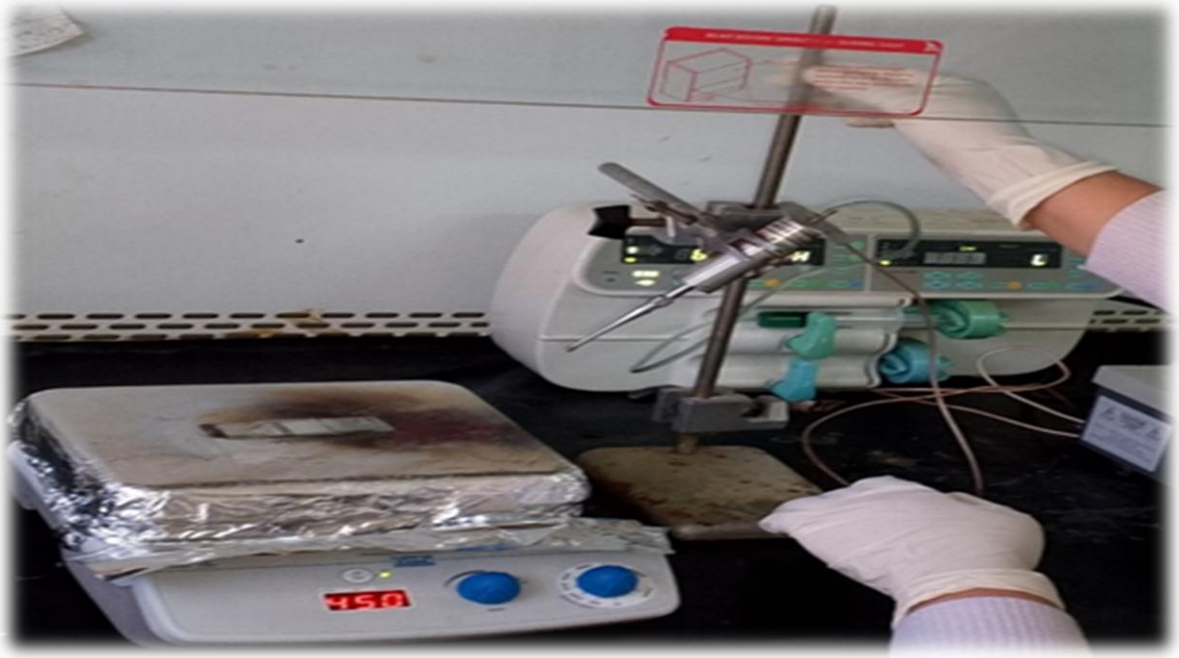
Effective mass of the electron in the conduction band	0.16-0.46 m_e
Effective mass of the hole in the valence band	0.54-3.7 m_e
Relative dielectric constant	12
Thermal conductivity (W K^{-1} m^{-1})	17

I.4.3.Applications of thin copper oxide

Copper oxide (CuO) is considered a promising material for various applications due to its low cost, simple composition, and excellent thermal stability. These properties, among others, have made CuO films a viable alternative in many important fields, including [75]:

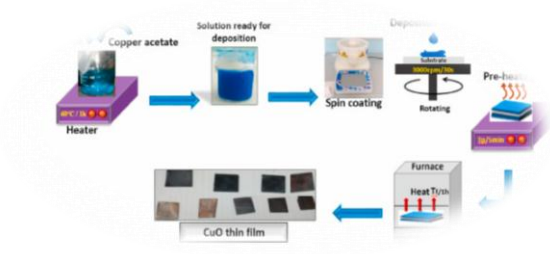
- **Solar energy applications:** Used in thermal and photovoltaic collectors, as well as in energy conversion systems.
- **Magnetic applications and magnetic energy storage.**
- **Gas sensing.**
- **Nanodevice fabrication:** The reduction in CuO temperature leads to the formation of materials with superconducting properties.
- **Optoelectronic applications:** Utilized in various devices such as light-emitting diodes (LEDs).
- **Lithium batteries:** Due to its high energy storage capacity and long-term usability.

it is relevant it is ok



Chapter II

Elaboration of copper oxide thin films









Chapter II: Elaboration of copper oxide thin films

This chapter consists of two parts. The first part explores the thermal decomposition technique using ultrasonic spray pyrolysis, including the steps for preparing undoped and chromium-doped copper oxide thin films. The second part focuses on studying the optical and electrical characterization methods of the prepared films.

Part one: Ultrasonic spray pyrolysis technique

II.1. Choice of ultrasonic spray pyrolysis technique

Ultrasonic Spray Pyrolysis (USP) is a simple and efficient technique for synthesizing nanomaterials, such as thin films and nanoparticles. It is characterized by its ease of implementation, flexibility, and low cost, making it an important alternative to chemical solution deposition (CSD). This method is widely used in electronic and optoelectronic applications due to its ability to produce large-area coatings with high stability compared to other techniques. It allows full control over several process parameters, including ultrasonic amplitude, precursor solution composition, viscosity, flow rate, and substrate temperature. This provides an advantage in producing dense or porous particles as well as thin film coatings. The technique was first introduced in 1959 when Hotle and Auger used it to prepare aluminum films using a benzene spray[76].

Since then, it has witnessed significant development, particularly in the field of semiconductors and optoelectronic applications [10,77].

II.1.1.Principle of Thermal Decomposition Deposition Technique

This technique relies on increasing the temperature of the material to be deposited to a certain degree, depending on the type of material[77]. Where the pyrolysis of volatile compounds occurs at the surface of the substrate. During this process, the substrate is heated to a temperature exceeding the decomposition temperature of the reactive materials, leading to their breakdown and the formation of films or coatings on the heated surface[78]. This process takes place in the air or under low pressure, typically within the range of (50 *torr*). It is possible to enumerate three methods to obtain thin films, which are: manual spraying, spraying by applying pressure to a solution, and spraying using ultrasonic vibrations[79].

The spray technique relies on dispersing solutions containing the desired elements and compounds onto a heated substrate. This is achieved using a spray gun with a fine nozzle, which, with the help of a carrier gas, converts the liquid into a fine mist[78].

The spray pyrolysis process goes through the following stages:

- Converting the solution or precursor material into fine droplets,
- Evaporating the solvent,
- Condensing the dissolved material,
- Decomposing and reacting the dissolved material,then
- Sintering the solid particles,

II.1.2. The advantages of spray pyrolysis technique

There are many advantages of the spray pyrolysis technique, including [17]:

- Spray pyrolysis is a distinguished technique for preparing metal oxide thin films.
- It is a simple, reproducible, and cost-effective method, making it suitable for large-area applications.
- The simple experimental setup allows easy observation of the deposition process and adjustments during the experiment.
- It features a high growth rate and large-scale production capability, making it useful for industrial and solar cell applications.
- This technique enables control over film morphology and particle size at the nanometer scale, resulting in high-quality thin films.

II.1.3. Factors affecting thin film preparation by ultrasonic spray pyrolysis technique

The principle of thin film formation by ultrasonic spray pyrolysis method depends on:

A. <u>Atomization rate and droplet size</u>

The size of the droplets is a crucial factor in the process (Figure II.1). If the droplets are too large, the heat will not be sufficient to convert them into vapor, leading to the formation of a solid (heterogeneous precipitate). On the other hand, if the droplets are too small, they will dry before reaching the target surface, causing the solvent to evaporate while the remaining substance settles, resulting in black spots on the surface due to material combustion. However, when the droplet size is moderate, which is the optimal condition for precipitation, the solvent partially evaporates before reaching the surface, allowing it to arrive as vapor. This enables the reaction to occur on the base, leading to the formation of the desired film[80].

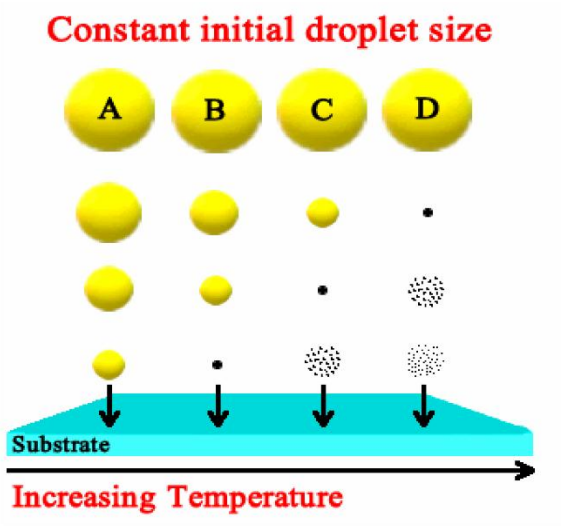


Figure II.1. Droplet size effect on the formation of thin films [81].

B. Thermal effects of the substrate on droplets

Figure II.2 illustrates the different stages a droplet undergoes as it approaches the hot substrate when the droplet size and speed remain constant while the substrate temperature increases [81].

- ✓ **Stage A:** The solvent inside the droplet is not completely evaporated. When the liquid droplet hits the hot substrate, the solvent evaporates upon contact, leaving a ring-shaped dry precipitate on the surface.
- ✓ **Stage B**: The solvent fully evaporates, leaving behind a dry precipitate (an amorphous precursor salt) that deposits on the substrate surface, where pyrolysis reactions take place.
- ✓ **Stage C:** The droplet undergoes all the previously mentioned stages. Near the substrate surface, the dry precipitates vaporize, leading to a chemical vapor deposition (CVD) reaction on the substrate surface.
- ✓ **Stage D:** At high temperatures, the vaporized precipitates undergo a chemical reaction in the vapor phase before reaching the substrate surface.

In the case of powder synthesis, similar processes occur. However, in this case, the key factor that controls the occurrence of different synthesis stages is the residence time of the droplet within the hot zone of the furnace[82].

hot plate

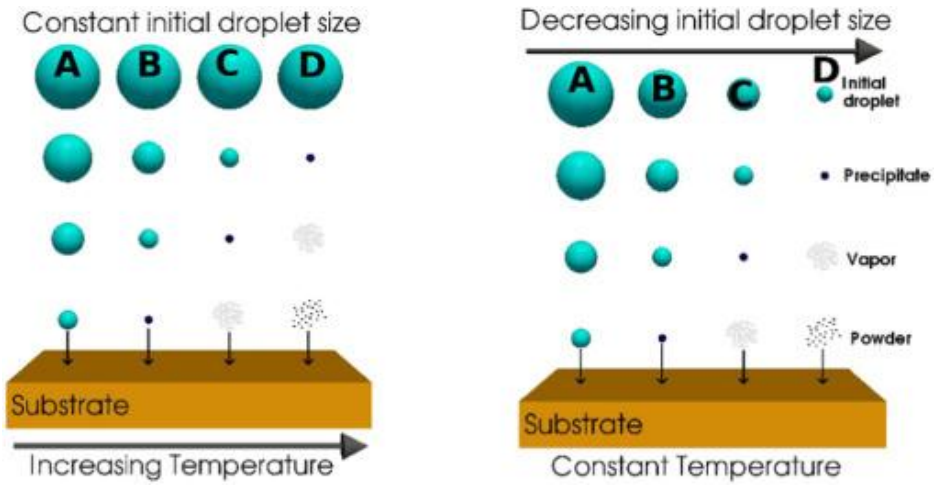


Figure II.2. Thermal effects of the substrate on droplets [81].

C. Effect of deposit time

The deposition time of thin films must be taken into account. When the spraying duration is long, the resulting film becomes thicker [83]. However, if the period is short, the formed film will be very thin, leading to weak atomic cohesion.

D. Effect of the nozzle-substrate distance

When the nozzle-to-substrate distance (D1) is small, spraying the solution containing various precursors results in a high-density droplet flow. This prevents the solution from transitioning into the vapor phase, causing it to remain in liquid form, which hinders the formation of a uniform layer on the substrate.

On the other hand, when the distance is relatively long (D3), the droplets formed after spraying the solution lead to the deposition of a powdery material on the substrate. This occurs because the droplets travel a long distance before reaching the substrate, affecting the quality of the deposition Figure II.3 illustrates the different stages a droplet undergoes at different nozzle-substrate distances (D1, D2, and D3) [84].

In contrast, a moderate nozzle-to-substrate distance (D2) has been found to produce high-quality deposits that adhere well to the substrate. This is because the appropriate distance allows the solution to pass through the required phases in the correct order, starting as a liquid, then gradually evaporating the solvent, which facilitates the effective deposition of the desired material and ensures strong adhesion of the thin film to the substrate [84].

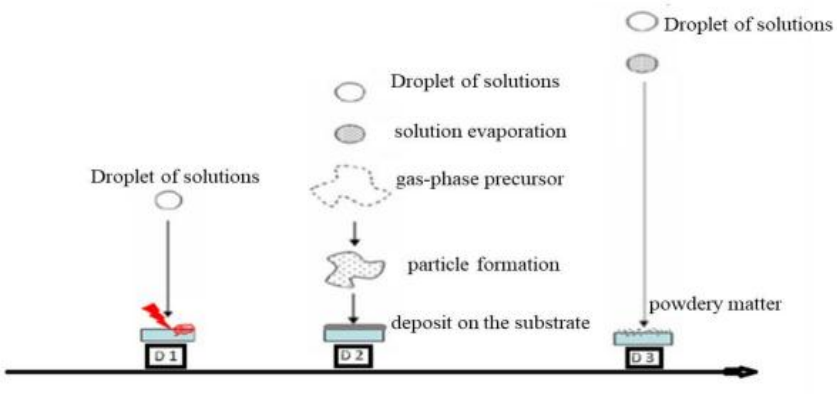


Figure II.3. Effect of Nozzle-substrate distance on film elaboration [84].

II.2. Experimental procedure

The objective of this work is to produce undoped copper oxide (CuO) and chromium-doped copper oxide (CuO:Cr) thin films using the ultrasonic spray pyrolysis technique at nozzle-substarate (d=5cm) , while keeping all other experimental parameters constant (deposition temperature, solution concentration, deposition time, nozzle-substrate distance, and solution flow rate). The study also investigates the effect of chromium doping and the annealing on the optical and electrical properties of copper oxide samples.

notation you use S

The precursor solutions used contain copper(II) chloride dihydrate ($CuCl_2$ $2H_2O$) and chromium(III) chloride hexahydrate ($CrCl_3$ $6H_2O$) dissolved in distilled water as a solvent.

II.3. Followed equipment

The experiment was conducted at the Laboratory of Materials and Structure of Electromechanical Systems and their Reliability (LMSSEF: Laboratoire des matériaux et structure des systéms électromécaniques et leur fiabilité) at Larbi Ben M'hidi University in Oum El Bouaghi. The undoped and chromium-doped copper oxide thin films were prepared using the ultrasonic spray pyrolysis technique, starting from simple elements (Figure II.4 and Figure II.5).



Figure II.4. Pyrolysis Spraying Device

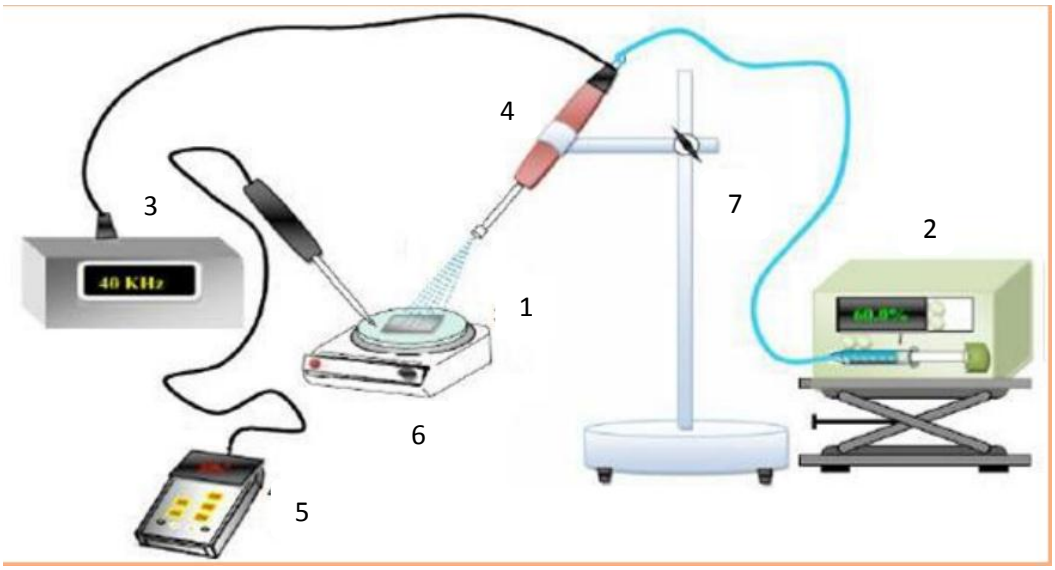


Figure II.5. The schematic experimental set up of the spray pyrolysis system [10].

1	2	3	4	5	6	7
The substrate	Electric syringe pump	wave generator (40 KHz) with an atomizer	The sprayer	Thermometer	Substrate heater	The holder

- Experimental setup :
  - ***The substrate:*** It is a glass slide or another material on which the film is deposited.
  - ***Thermometer:*** measures temperature.
  - ***Substrate heater:*** It is a resistor connected to an electrical circuit that operates by the Joule effect.

- ***The sprayer:*** Under pressure, it allows the initial solution to be converted into a jet of very fine droplets, through which the substrate is sprayed with the solution.
- ***Compressor:*** It allows the carrier gas (in our case, air) to be pressurized at a controllable pressure, which drives the solution to the nozzle[85].
- ***Ultrasonic wave generator (40 KHz) with an atomizer:*** Which allows to transform the solution at the level of the atomizer to very small droplets and fine thin.
- ***Electric syringe pump:*** Model PHOENIX D-CP (GF-FOURES) to control the precursor solution flow rate[10].

II.4. Stages of preparation thin films

II.4.1. Choice the substrate

Glass was chosen as the substrate based on the following criteria [68] :

1. Coefficient of thermal expansion: $\alpha_{Glass} = 8.5\times10^{-6}K^{-1}$ and $\alpha_{CuO} = 48\times10^{-6}K^{-1}$.

2. Low cost.

3. Transparent, allowing optical characterization of thin films in the UV-visible-NIR range.

4. Provides good adhesion, improved structure, and better piezoelectric activity.

For thin film deposition, glass microscope slides with dimensions (76.2 × 25.4) mm and a thickness of 1 mm were used. Each slide was cut into three substrates using a diamond tip pen **(Figure II.6).**



Figure II.6. Glass microscope Slides (substrates).

- After obtaining the substrates, they must be cleaned according to the following basic steps (Figure II.7):

- Rinsing with distilled water.
- Soaking in an acetone bath.

- Rinsing again in a distilled water bath to remove any acetone residues.
- Soaking in an ethanol bath.
- Washing with distilled water to remove any remaining ethanol traces.
- Finally, these substrates are dried using Joseph papers .

The degreasing process in each bath lasts five minutes at room temperature in an ultrasound cleaning bath (Figure II.7).



Figure II.7. Substrate cleaning steps with some used tools.

II.5. Preparation of deposition solutions

a.Preparation of copper(II) chloride colution

There are several sources of copper such as: copper hydroxide ($Cu(OH)_2$), copper nitrate ($Cu(NO_3)_2$) and copper sulfate ($CuSO_4$) [86]. In this work, copper (II) chloride dihydrate ($CuCl_2 \cdot 2H2O$)was used as a source of copper material (Figure II.8).



Figure II.8. Copper(II) Chloride dihydrate.

Table II.1. Some physical properties of $CuCl_2$ [68].

Appearance	Crystalline solid
Color	Bright greenish-blue crystals
Molecular formula	CuCl2 2H2O
Molar mass (g/mol)	170.48
Density (g/cm^3)	6.32
Melting point (°C)	100

To prepare a solution of copper(II) chloride dihydrate (CCD) (V) with a molar mass of 170.48 g/mol and a concentration of C = 0.05 mol/L, a quantity of copper(II) chloride ($m_{CCD}=C\times M_{CCD}\times V$) was dissolved in distilled water (Figure II.7). A KERN442-432N balance with an accuracy of ±0.01 g was used to weigh a specific amount of copper(II) chloride (m_{cucl2}). We influence the solution for 5 min with ultrasonic waves to obtain a homogeneous solution using ultrasonic cleaner device.

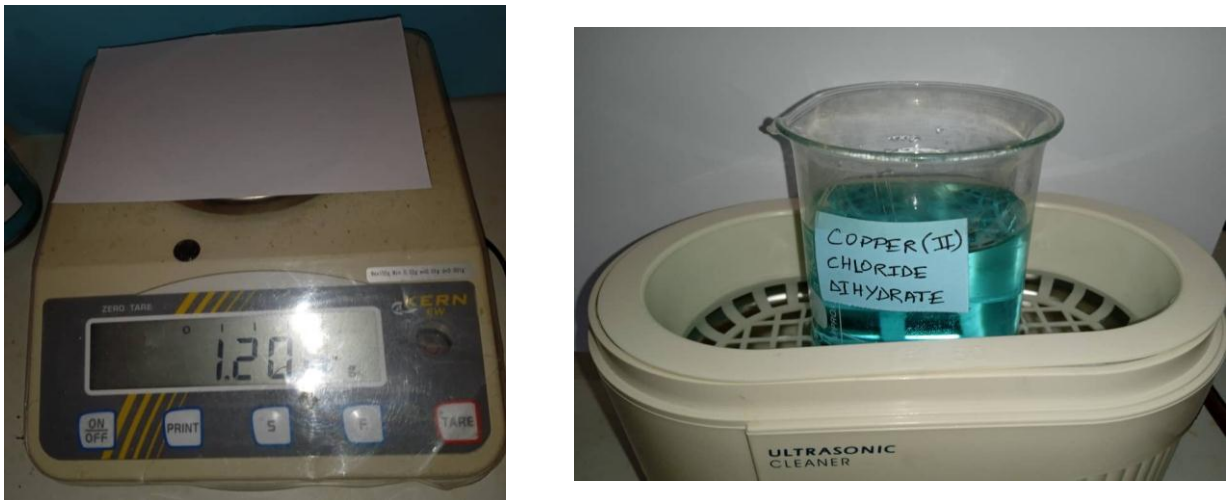


Figure II.9. Preparation of Copper(II) Chloride dihydrate solution.

We influence the solution for 5 min with ultrasonic waves to obtain a homogeneous solution using ultrasonic cleaner device.

b. Preparation of chromium chloride solution

In this study, chromium chloride hexahydrate ($CrCl_3.6H_2O$) was used as a source of chromium material (Figure II.10).



Figure II.10. Chromium chloride hexahydrate.

Table II.2. Some physical properties of (CrCl3 · 6H2O) [9,87,88,89].

Appearance	Crystalline solid
Color	Dark green
Solubility in water at 20°C (g/100ml)	59
The molecular formula	$CrCl_3 \cdot 6H_2O$
Molar mass (g/mol).	266.5
Density at 20°C (g/cm^3)	2.76
Melting point (°C)	83-95

To prepare a solution of chromium chloride hexahydrate (CrCH) with a molar mass of 266.5 g/mol and a concentration of C=0.05 mol/l, a specific quantity of chromium chloride hexahydrate ($m_{CrCH}=C_{CrCH}.M_{CrCH}.V$) was dissolved in distilled water (Figure II.11). The previous balance was used to weigh the required amount of CrCH.

We place the solution in an ultrasonic device to obtain a homogeneous solution.

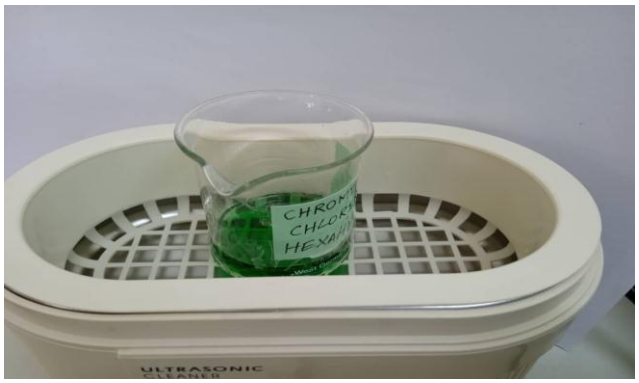


Figure II.11. Preparation of chromium chloride hexahydrate solution.

We observe that chromium chloride hexahydrate dissolves well and completely in water, resulting in a homogeneous solution with a green color especially after exposure to ultrasonic waves for 5 min using ultrasonic cleaner device.

c. Preparation of precursor solution

After preparing the two solutions, a specific amount of copper chloride dihydrate solution is mixed with a determined amount of chromium chloride hexahydrate solution to prepare a precursor solution used for producing samples of chromium-doped copper chloride with a doping ratio of (Z)% where :

Experimental condition

To study the effect of chromium-doping on the copper oxide (CuO:Cr), several samples were prepared according to the experimental conditions presented in the table.

Table II.3. Precipitation Conditions of Copper Chloride (CrCl3 · 6H2O).

Conditions	Values
Nature of precursor	$CuCl_2 \cdot 2H_2O$ $CrCl_3 \cdot 6H_2O$
Solvent	H2O
Molarity of the solution (mol/l)	0.05
Volume of soution for each deposit (ml)	40
Substrate temperature (°C)	350
Solution folow (ml/h)	60
Deposition time (min)	4
Doping rate (at. %)	0 , 3 , 6 , 9 , 12

II.6. Deposition of thin film

To prepare the thin films under study, we follow these steps:

Initially, all doped solutions with different concentrations (3%, 6%, 9%, 12%) are prepared in addition to the basic solution (0%), as shown in (Figure .II.12.a).

- First,To ensure the proper growth of thin films, all devices are checked for readiness and safety before starting the process.

- Second,The substrate is placed above an electrical resistor and gradually heated from room temperature up to the deposition temperature (T_s = 350°C) to prevent thermal shock to the substrate.
- Third,once the heating process is complete, the precursor solution to be deposited is placed in syringe (Figure .II.12.b), which is then mounted on a syringe pump device. The flow rate is set to 60 mL/h to ensure a slow and controlled flow of the solution. The ultrasonic generator breaks the solution into fine droplets that disperse near the vapor.
- Finally, the deposition process is carried out by spraying the solution onto the hot substrate for 4 minutes (Figure .II.12.c).
- After that, the heating is stopped, and the substrates are left to cool gradually to room temperature, preventing thermal shock that could cause sample cracking. Once cooled, the samples are recovered, and it was observed that the deposited films well-adhered to the glass substrates and nearly transparent compared to the color of CuO film.

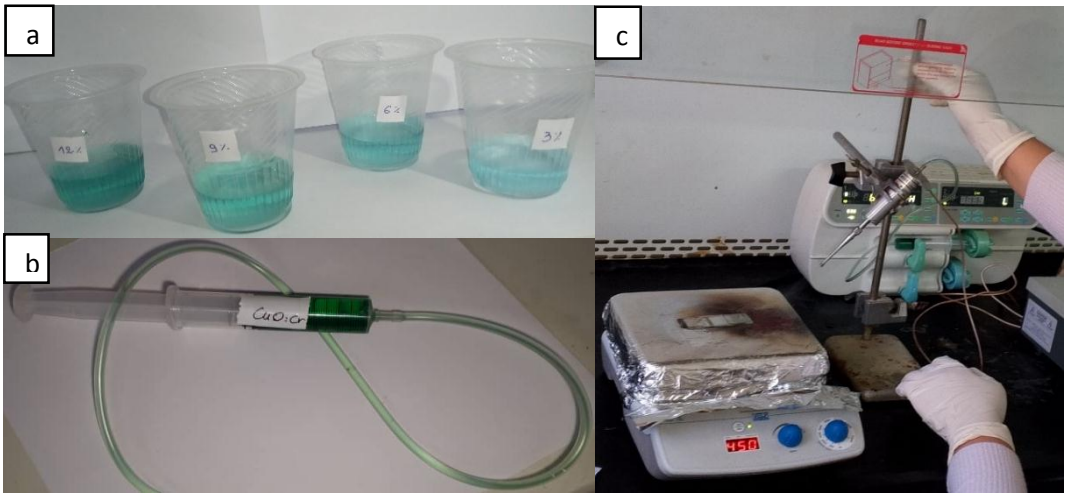


Figure II.12. Deposition of thin film; **a.** doped solutions, **b.** the syringe, **c.** spraying the solution**.**

II.7.Annealing of deposited samples

After the preparation of the samples, thermal treatment was carried out using a small electric heating device (Figure II.13) instead of a conventional furnace. This device enables direct heating of the samples while exposing them to ambient air, allowing simultaneous thermal treatment and oxidation. The process was performed at a temperature of 350°C for a duration of one hour (*1h*)

During this treatment, the samples undergo oxidation, leading to the transformation of cuprous oxide (Cu_2O) into cupric oxide (CuO) according to the following reaction [7]:

$$2Cu_2O + O_2 \xrightarrow{Heat} 4CuO \qquad \text{(II.1)}$$

Although the ideal reaction occurs at, the temperature used in our experiment *(350°C)* is sufficient to initiate the oxidation process, enhance the crystallinity of the thin films, and improve their thermal stability. This treatment contributed to the improvement of the structural, optical, and electrical properties of the samples, with precise temperature control ensured by the device's regulator[7].



Figure II.13. Picture of an electric heating device.

Part two: Characterization techniques of thin films

After the preparation and the annealing of thin films, their optical and electrical properties are studied to obtain various information about the prepared sample.

II.1. Optical characterization of thin films

The characterization methods of transparent conductive oxide thin films vary, as there are numerous structural, electrical, and optical techniques used to determine the properties of these films. These methods help in studying the characteristics of the deposited thin films, such as band gap, absorption coefficient, refracive index, thickness, and film types. These properties are obtained by analyzing the transmission spectrum (optical transmittance curve as a function of wavelength) using a UV-Vis Spectrophotometer[16].

II.1.1.Ultraviolet-visible spectroscopy

Spectrophotometric measurement technology within ultraviolet-visible-Near Infrared (UV-Vis-NIR)spectrum is used to analyze the optical properties of thin films (Figure II.14). This technique is an effective tool for determining the optical characteristics of materials. It relies on measuring changes in light intensity after passing through the sample, where the material absorbs light within a specific wavelength range, leading to the excitation of electrons and their transition from lower to higher energy levels. The absorption range of ultraviolet-visible radiation extends from 200 to 350 nm for ultraviolet light , 350-800 nm for visible light light, and 800 to 1100 for IR light.. Figure (II.15) illustrates the operating principle of the spectrophotometer used in this technique. A light beam emitted from the UV-VI source is directed at two mirrors; the first reflects part of the beam, while the remaining portion passes through the sample. The transmitted beam is then detected by a photodetector, and the data is analyzed using computer software for result processing. The physical properties of thin films can be studied using UV- Vis-NIR spectrophotometric analysis. The resulting curve provides information on variations in spectral absorption concerning different wavelengths, allowing us to deduce key characteristics such as film thickness, absorption coefficient, optical absorption edge, energy gap, and refractive index[90].

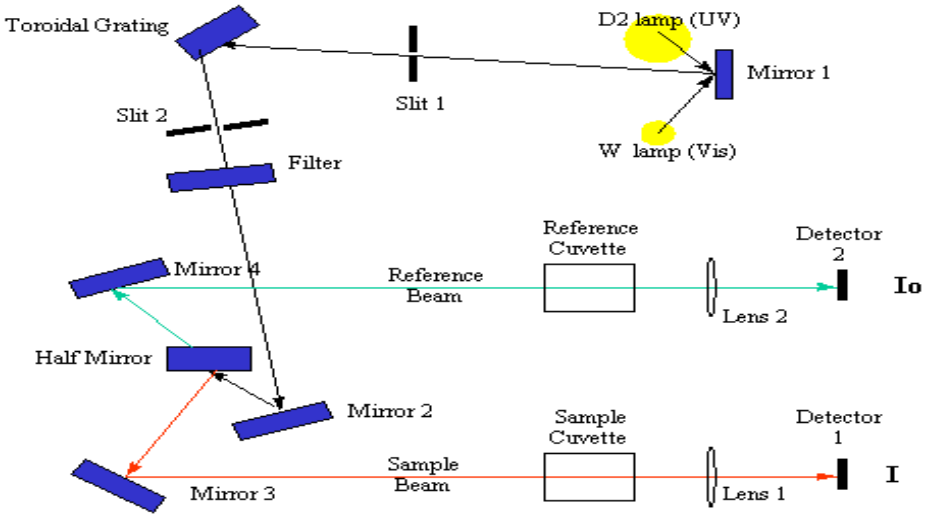


Figure II.14. Principe of measure the transmission UV-Vis-NIR [91].



Figure II.15. Experimental device for UV-Vis-NIR spectroscopy.

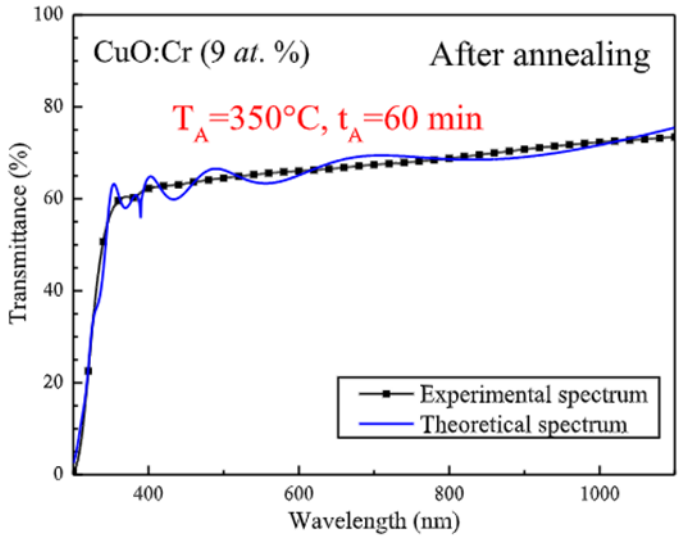


Figure II.16. Transmittance Spectrum of CuO:Cr (9 at.%) Thin Film After Annealing at 350°C.

This figure illustrates the transmittance spectrum of a chromium-doped copper oxide (CuO:Cr 9 at.%) thin film after annealing at a temperature of 350°C for 60 minutes. The curve shows that transmittance is initially low at short wavelengths, then rises sharply starting from a wavelength of 325 nm, reaching values of approximately 85% in the visible region (400–800 nm).

This behavior indicates a clear improvement in the film's transparency as a result of the annealing process, reflecting enhanced structural quality and reduced defects. The good agreement between the experimental and theoretical spectra suggests that the thin film is homogeneous and optically stable. Accordingly, the sample doped with 9% chromium is well-suited for optical applications, particularly in solar cells, as it allows a significant amount of light in the visible range to pass through, thereby improving solar energy absorption and conversion efficiency[44,90].

II.1.1.1. Determination of film thickness and refractive index

The thickness and refractive index of the film can be determined through the transparency curve, which can be divided into two regions, each related to the wavelength. This curve contains several constants, including thickness and refractive index. Using the least squares method, the best fit for the data can be obtained (Figure II.16). Based on calculus and linear algebra, the main problem is to find the mathematical relationship such that the values are available for the set . The least squares regression method is used to predict the behavior of the dependent variable. The thickness and refractive index of copper(II) chloride films doped with chromium chloride are determined from transmission spectra using the Fit software, which allows for changing the number of parameters. The least squares method is also used to adjust the simulated transmission curve to the measured values[53].

II.1.1.2. Determination of absorption coefficient

When the UV-Visible-NIR spectrum passes through the sample, part of the radiation is absorbed by the thin film, while another part is transmitted. Using these relationships, the absorption coefficient can be calculated as a function of wavelength, allowing for the analysis of the optical properties of thin materials.

The calculation of the absorption coefficient is based on the transmitted spectrum through thin films. This is done using the Beer-Lambert law, which is given by the equation:

$$T = (1 - R)e^{-\alpha d} \quad \text{(II.2)}$$

α : the absorption coefficient.

d : the film thickness.

R : the reflectance (which can be neglected in some cases).

When reflectance is neglected, the optical transmittance becomes:

$$T = e^{-\alpha t} \quad \text{(II.3)}$$

From this equation, the absorption coefficient can be determined using the following formula [10,90]:

$$\alpha = \frac{1}{d} \ln \left(\frac{100}{T(\%)}\right) \quad \text{(II.4)}$$

II.1.1.3.Determination of optical band gap

The UV-Vis-NIR spectrophotometer was used to analyze the amount of light that the copper oxide (CuO:Cr) thin film can absorb. The initial absorption, which corresponds to the excitation of electrons from the valence band to the conduction band (Figure II.17), is analyzed using the Tauc plot method to determine the optical band gap of the manufactured film. The following equation describes the relationship between the absorption coefficient (α) and the incident photon energy (hν)[70]:

$$(\alpha h\nu)^n = K\,(h\nu - E_g) \quad \text{(II.5)}$$

where:

E_g : represents the band gap energy.

α : is the absorption coefficient.

K : is the proportionality constant.

hν : denotes the energy of the incident photon.

n : takes the value 2 for a direct band gap and ½ for an indirect band gap.

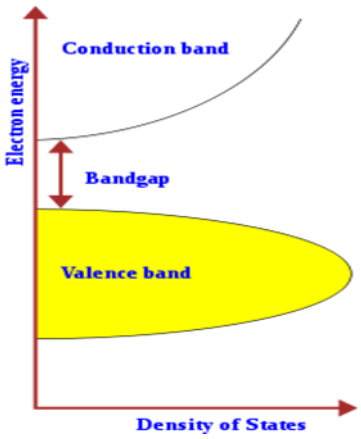


Figure II.17. Explanation of band gap [92].

The band gap is determined by analyzing the slope of the straight-line plot of $(\alpha h\nu)^2$ versus $h\nu$. This plot, as shown in Figure II.18 , indicates that the absorption is due to a direct allowed electronic transition. The optical band gap (E_g) is extracted from the point where the extrapolated straight line intersects the $h\nu$ axis.

For the CuO:Cr(* at. %) thin film prepared using ultrasonic spray pyrolysis method, the optical band gap was evaluated at 1.48 eV, which falls within the reported range of 1.21 eV to 1.51 eV for copper oxide. The reduction in band gap may be attributed to an increase in film thickness, enhancing its potential application as an absorber layer in solar cell fabrication[70].

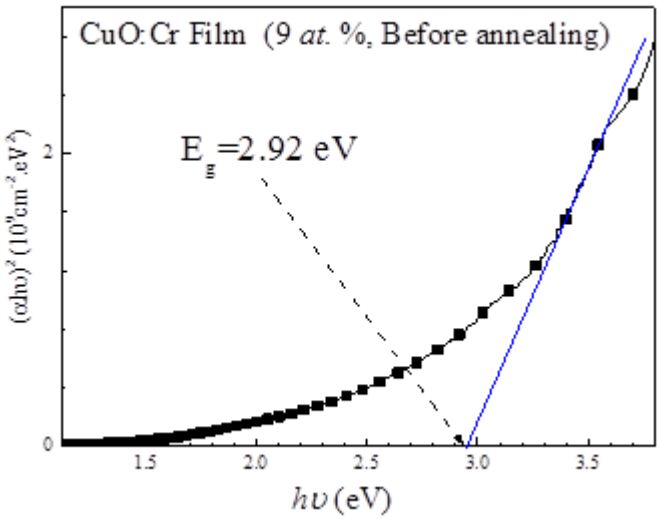


Figure II.18. Band Gap Determination of CuO:Cr Film Before Annealing

II.1.1.4. Determination of Urbach Energy

Urbach energy is one of the key properties of thin films, reflecting their ability to absorb light. The relationship between Urbach energy and the absorption coefficient is expressed by the equation II.6 :

$$\alpha = \alpha_0 \exp\left(\frac{h\nu}{E_{Urb}}\right) \quad \text{(II.6)}$$

This relationship can also be rewritten using the natural logarithm of the absorption coefficient as follow [90]:

$$ln\alpha = \left(\frac{1}{E_{Urb}}\right) h\nu + ln\alpha_0 \quad \text{(II.7)}$$

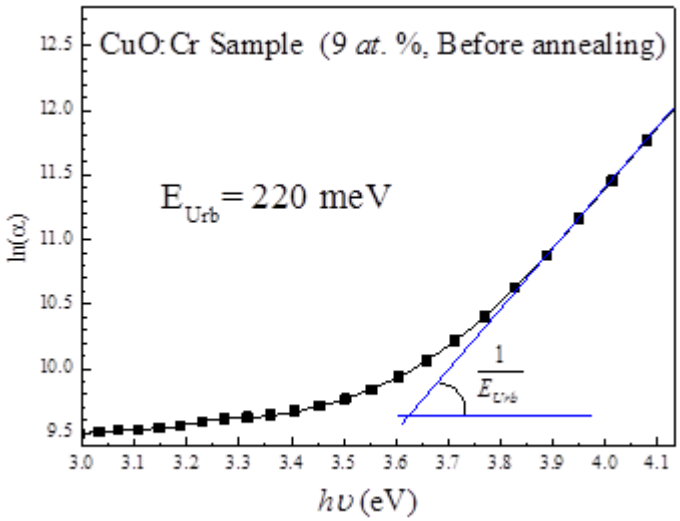


Figure II.19. Urbach energy Determination of CuO:Cr Film Before Annealing

II.2. Electrical characterization of thin films

Electrical properties cover a broad field, and the electrical characteristics of thin films are among their most significant physical features, particularly conductivity and resistivity[36]. To ensure accurate measurement of the resistance of the manufactured layers, a four-terminal sensing method was applied .

The four-point probe technique is used to measure the sheet resistance of thin films and determine their electrical condictivity. This is achieved using a device consisting of four equally spaced probes(Figure II.21). The outer probes supply the current, while the inner probes measure the voltage difference.

Since the current distributes across the thickness of the sample, the spacing between the probes should be significantly larger than the film thickness to ensure accurate measurement.

Additionally, the sample is considered an infinite conductive medium due to its unbounded edges, which simplifies the calculation of sheet resistance based on physical laws[93].

The relationship between voltage, current, and sheet resistance is expressed using the following equation:

$$k = \frac{I.\rho_S}{V} \quad \text{(II.8)}$$

where:

ρ_S: Represents the sheet resistance of the thin film and is given as a function of material's resistivity (ρ) by the equation $\left(\frac{\rho}{d}\right)$

K: A proportionality constant, equal to $\frac{\pi}{\ln 2}$

By substituting these values, we obtain the following formula, which allows for calculating the sheet resistance:

$$\rho_S = \frac{\pi}{ln2}\left(\frac{V}{I}\right) \quad \text{(II.9)}$$

Since the film thickness (d) is known from the optical transmittance measurements[24], the material electrical conductivity (σ) can be calculated:

$$\sigma = \frac{1}{\rho_S\, d} \quad \text{(II.10)}$$

To determine the electrical conductivity (σ) of chromium-doped copper oxide thin films, a four-point probe device of the Jandel type was used in the LMSSEF laboratory at Larbi Ben M'hidi University in Oum El Bouaghi (Figure II.20). This probe consists of four electrodes aligned in a straight line, with a spacing of 1 mm (S = 1 mm) between them. A variable current (I) is applied through the outer electrodes, while the voltage (V) is measured between the inner electrodes using a Keithley 2400 measurement device, allowing for accurate detection of low voltages.



Figure II.20. Four-point probe + keitheley 2400 Source Meter.

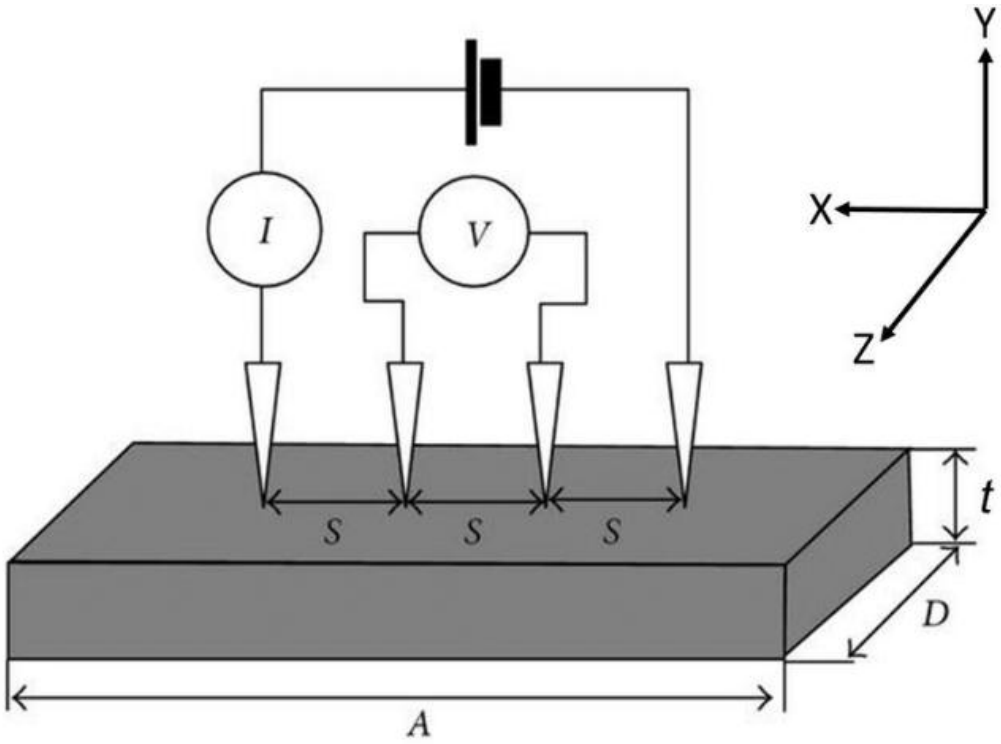
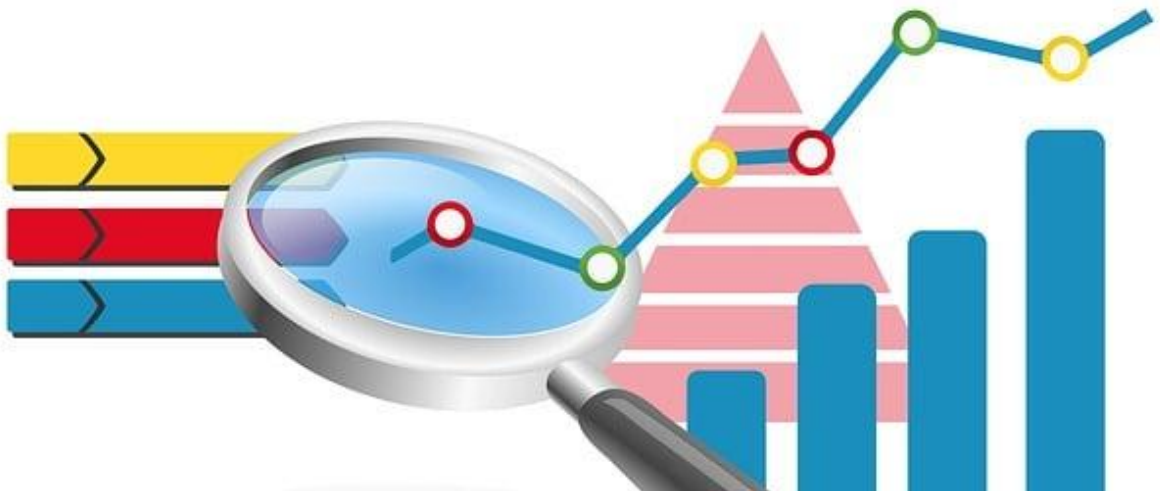


Figure II.21. Diagram representative of the principle of the four-point probes method [64].

Chapter III

Results and discussion



Chapter III: Results and discussion

The purpose of this chapter is to present and interpret the experimental results of this work on the development and characterization of thin films of undoped and chromium-doped copper oxide (CuO:Cr) deposited on glass substrates using the ultrasonic spray pyrolysis technique.

In this chapter, the optical and electrical properties of copper oxide thin films and the effect of chromium doping (CuO:Cr) at different atomic concentrations (0, 3, 6, 9, and 12 at. %) and the effect of annealing under constant deposition (T_s, t_D, and φ_S) and annealing conditions (T_A, t_A) are presented .

Two techniques were used to characterize the samples as follows:

- UV-Vis-NIR spectrophotometry was used to analyze the transmittance spectrum and to calculate: the film thickness (d), the absorption coefficient (α), the optical band gap energy (E_g), the Urbach energy (E_{Urb}), and the refractive index (n) of the films.
- The four-point probe techniques was used to measure the electrical conductivity of the samples.

III.1Photos of CuO :Cr samples

Table III.1. Photos of CuO :Cr thin films deposited on glass substrates.

	Bare substrate	0 *at.* %	3 *at.* %	6 *at.* %	9 *at.* %	12 *at.* %
Before annealing						
After annealing						

Table III.1 presents images of the prepared CuO:Cr samples, where it is observed that the color change is barely noticeable, as the samples appear nearly transparent when exposed to visible light. This is attributed to the fact that copper oxide, whether undoped or doped with elements such as chromium, exhibits low transparency within this range of the spectrum [94].

III.2 Optical characterizations

III.2.1. Effect of Cr-doping and annealing on the optical transmittance of CuO samples

A UV-Vis-NIR spectrophotometer (model JASCO V-630) was used to analyze the optical properties of the prepared samples. This device enabled us to record spectra illustrating the changes in optical transmittance of the CuO:Cr samples across the wavelength range extending from ultraviolet to near-infrared, as shown in figure III.1.

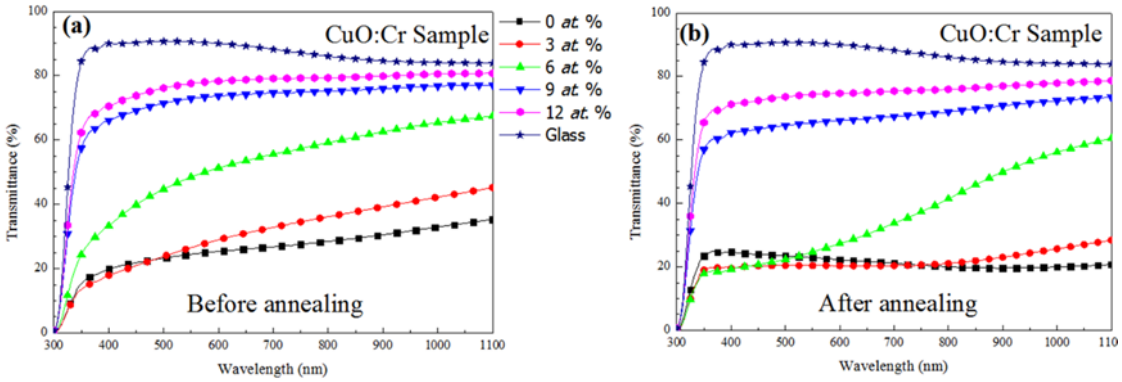


Figure III.1. Optical transmittance spectra of CuO samples doped with different concentrations of Cr **(a):** before annealing **(b):** after annealing.

The graphs illustrate the variation in optical transmittance (%) with wavelength for CuO:Cr samples before and after annealing doped with different concentrations of chromium (0 *at.* %, 3 *at.* %, 6 *at.* %, 9 *at.* %, and 12 *at.* %), along with glass used as a reference . Before annealing, glass shows the highest transmittance, reaching around 85–90% in the visible, which is expected due to its transparency. As the Cr concentration in CuO increases, the transmittance also increases gradually, with the sample containing 12 *at.* % Cr exhibiting the highest transmittance among the doped samples.

After annealing , a decrease in the transparency of the samples was observed compared to their state before treatment. This reduction is attributed to the reorganization of the material caused by the presence of copper oxide (CuO), which is less transparent than chromium (Cr). It is not due to the glass used, as glass is not affected by heat treatment (Figure III.2.a).

At concentrations of 0%, 3%, and 12%, a noticeable improvement in sample transparency was observed, indicating better structural organization of the material. In contrast, the 9% sample maintained a similar level of transparency in the visible range, showing no significant change. However, the 6% sample showed a considerable decrease in transparency due to its darker color after heat treatment, which negatively affects light transmission in the visible spectrum compared to the other samples.

CuO itself is a semiconductor with a narrow band gap compared to chromium oxide (Cr_2O_3), which relatively causes strong light absorption in the visible region [77]. The introduction of chromium modifies the band gap slightly, leading to reduced absorption and increased optical transmittance. These findings suggest that careful control of Cr doping and post-processing treatments like annealing can significantly enhance the optical properties of CuO:Cr thin films for potential use in optoelectronic applications . It was observed from Figure III.2.b that the permeability of the Cr_2O_3 sample did not affected by annealing at 350°C.

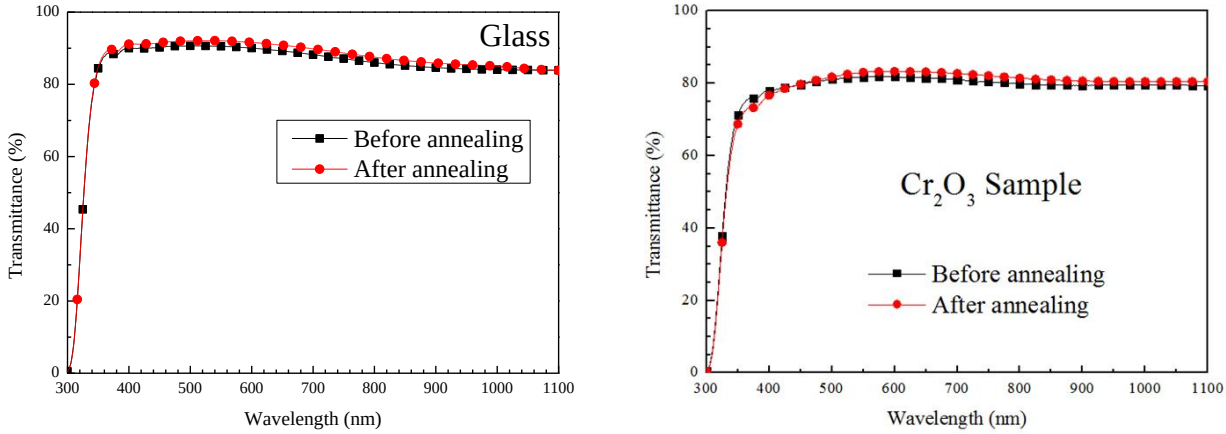


Figure III.2. Effect of annealing on the optical transmittance of glass and Cr_2O_3 sample.

Figure III.3 (a and b) shows typical curves of the variation in optical transmittance of CuO:Cr thin films using the ultrasonic spray pyrolysis technique as a function of the incident photon wavelength within the spectral range from ultraviolet to near-infrared (UV-Vis-NIR), covering the range from 300 to 1100 nanometers.

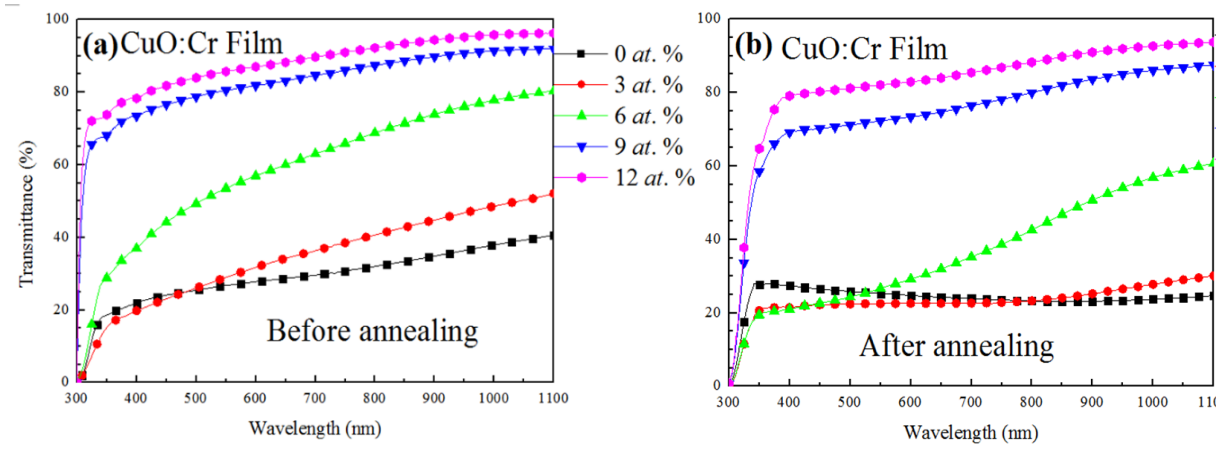


Figure III.3. Optical transmittance spectra of CuO:Cr thin films at different percentage of Cr **(a):** before annealing **(b):** after annealing.

The curve (a) before annealing shows that the optical transmittance of CuO:Cr films clearly varies with the chromium (Cr) doping ratio. The film with 0 at.% Cr exhibits the lowest transmittance, exceeding 40% at 1100 nm, while transmittance gradually increases as the Cr content increases, reaching its highest value at 12 *at*.%. This increase can be attributed to the lack of structural defects or scattering resulting from the irregular film structure. After annealing, as shown in curve (b), A noticeable decrease in light transmittance was observed in all samples. , especially the sample containing 6% chromium, which is consistent with explanations related to increased light absorption due to the lower transparency of CuO compared to Cu_2O, as well as the change in color, as it became darker after annealing.

Additionally, the presence of voids and gaps on the film surface before annealing, and the microscopic scattering resulting from a rough surface structure, are mitigated post-annealing as the layers become more compact and smooth, leading to decreased transmittance. Comparing performance before and after annealing, it is evident that annealing significantly enhances transmittance.

III.2.2.The effect of doping and annealing on the thickness of CuO:Cr film

The average thickness of the films were calculated by analyzing the variation in optical transmittance as a function of the incident photon wavelength within the UV-Vis-NIR range, using the least squares method as explained in chapter II.

mentionned

Figure III.4. represents the variation in the average thickness before and after annealing of CuO:Cr films with different chromium doping levels ranging from 0 *at*. % to 12 *at*. % .

The results show that the average thickness of chromium-doped copper oxide films, both before and after annealing, is higher compared to that of undoped copper oxide films. Additionally, the thickness increases from around 370 nm to over 400 nm before annealing.

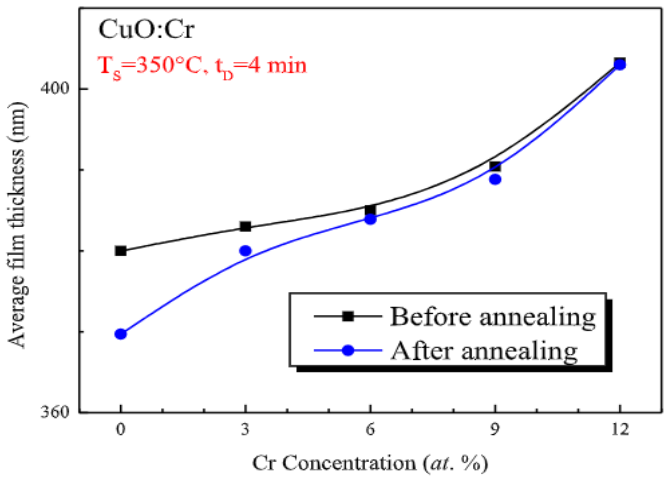


Figure III.4. Variation in the average thickness before and after annealing of CuO:Cr with different doping levels.

This increase in thickness can be attributed to several factors. First, there is a rise in porosity within the deposited material. It is well known that there is a direct relationship between porosity and thickness, as higher porosity contributes to greater apparent thickness.

Second, during doping, the Cu content was reduced while the proportion of Cr was increased. Through theoretical calculations, it was found that this substitution increases the oxygen content in the material, which in turn leads to an increase in the lattice constant. As a result of this lattice expansion, the sample thickness increases significantly.

After annealing, the measured thickness slightly decreases compared to the pre-annealing values at the same doping levels. This reduction is due to recrystallization and improvement in the crystalline structure of the film, which leads to reduced porosity and consequently lower average thickness.

Several studies have confirmed that the introduction of dopant elements during film growth generally results in an increase in thickness, regardless of the deposition method or the type of dopant material. These findings demonstrate that both chromium concentration and annealing significantly affect the growth behavior and thickness of CuO:Cr films, allowing for controlled tuning of film properties based on the desired application[64].

III.2.3.Effect of chromium doping and annealing on the optical absorption of CuO thin films

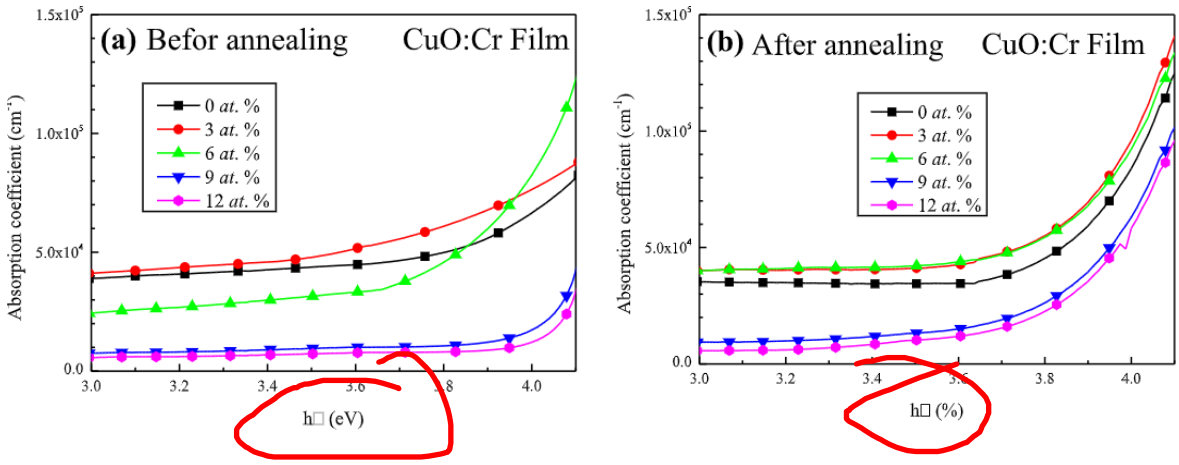


Figure III.5. The optical absorption of CuO:Cr films at different chromium concentrations **(a)** before annealing and **(b)** after annealing.

The figures III.5 show the relationship between the absorption coefficient and photon energy for chromium-doped copper oxide (CuO:Cr) thin films, both before and after annealing. Before annealing, increasing the chromium concentration from 0% to 12% leads to a gradual

decrease in the absorption coefficient. The highest absorption is seen in the undoped sample (0%), while the lowest is observed at the highest doping level (12%). This decrease is attributed to the increased transparency of the material and the higher porosity resulting from the increased doping level, which leads to the formation of more voids in the structure and consequently reduces the material's light absorption capability.

After annealing, a noticeable effect in the absorption coefficient is observed in all samples. Annealing enhances the crystalline structure and reduces defects, leading to better optical performance.

Overall, annealing plays a crucial role in enhancing the absorption characteristics of CuO:Cr thin films, with the optimal doping range found to be between 3% and 6%. Additionally, the absorption coefficient increases with increasing photon energy and reaches a maximum value of 1.5×10^5 cm^{-} at 4.13 eV, indicating excellent light absorption capability at higher photon energies.

III.2.4. The effect of doping and annealing on the Urbach energy of CuO:Cr

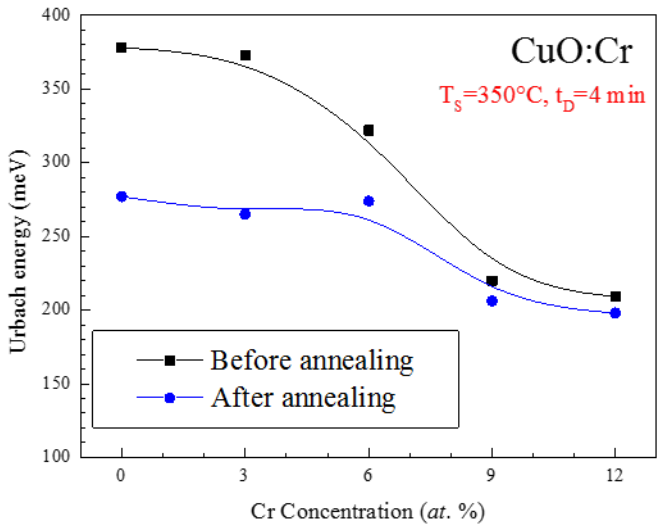


Figure III.6. Variation of Urbach energy of CuO:Cr thin films before and after annealing.

The figure III.6 illustrates the influence of chromium (Cr) doping on the Urbach energy (E_{Urb}) of copper oxide (CuO) before and after annealing. It is observed that the Urbach energy values are high at low chromium concentrations and progressively decrease with increasing doping levels. This behavior can be explained by the introduction of Cr atoms into the CuO lattice at interstitial sites,which gradually improves the crystalline structure by reducing copper vacancies in the lattice, leading to a decrease in E_{Urb}.

After annealing, a further reduction in E_{Urb} is observed compared to the pre-annealing state. This can be attributed to the recrystallization process during annealing, which promotes the elimination of defects and impurities, improves stoichiometry, and reduces porosity and surface roughness. As a result, the films become denser and more structurally ordered, which contributes to a general decrease in the Urbach energy. This change confirms that both chromium doping and annealing play a complementary role in enhancing the structural properties of CuO thin films.

III.2.5.The effect of doping and annealing on the optical band gap of CuO:Cr

By relying on the optical process described in Chapter II, the optical bandgap energy (Eg) values were calculated for undoped and chromum-doped copper oxide before anf after annealing.

As a reminder, the optical bandgap is defined as the energy range in which no electrons are present. It represents the energy difference between the top of the valence band and the bottom of the conduction band[95].

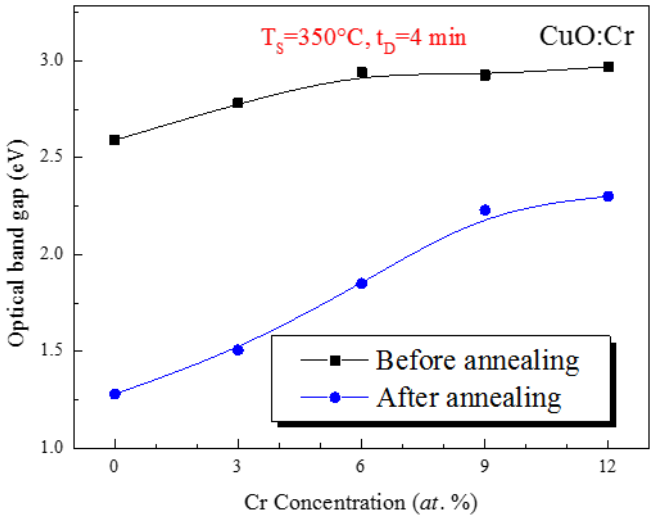


Figure III.7. Variation of the optical band gap energy of copper oxide thin films doped with chromium before and after annealing.

Figure III.7 shows the variation in the optical band gap energy (Eg) of chromium-doped copper oxide (CuO:Cr) thin films as a function of chromium atomic concentration (*at*.%), before and after annealing at 350°C for 1 hour. From the curve, it can be observed that the optical band gap energy increases progressively with increasing chromium concentration from 0% to around 12%, both before and after annealing. Before annealing, higher Eg values were recorded, exceeding 2.5 eV, which is attributed to the improvement in crystallinity and the

reduction in defect density with increased incorporation of chromium ions into the CuO lattice. It is noteworthy that the band gap energy of chromium oxide (Cr_2O_3) ranges between 3.4 and 3.5 eV, and therefore, doping CuO with chromium—either before or after annealing—leads to an increase in Eg due to the contribution of Cr to raising the average band gap energy.

After annealing, a general decrease in Eg values was observed, whatever the chromium concentration in the copper oxide lattice. This decrease is mainly attributed to the increase in grain size resulting from recrystallization during the annealing process, which reduces quantum confinement effects and thus narrows the optical band gap. Furthermore, the thermal treatment led to a phase transformation from Cu_2O to CuO. Since Cu_2O has a larger band gap than CuO, this transformation contributes to the observed reduction in the optical band gap after annealing. The presence of additional oxygen during annealing also leads to the formation of more CuO phase, which results in a decrease in transparency. Therefore, the drop in the transmittance curve after annealing can be attributed to the formation of the CuO phase.

Thus, it is clear that both chromium concentration and thermal treatment significantly affect the optical properties of the CuO thin films.

Figure III.8 illustrates the behavior of the optical band gap and Urbach energy for CuO:Cr films before or after annealing.

An inverse relationship between the Urbach energy (E_{Urb}) and the band gap (E_g) has been observed.

This behavior can be explained by the addition of chromium into the CuO lattice which reduces the density of localized states within the band gap.

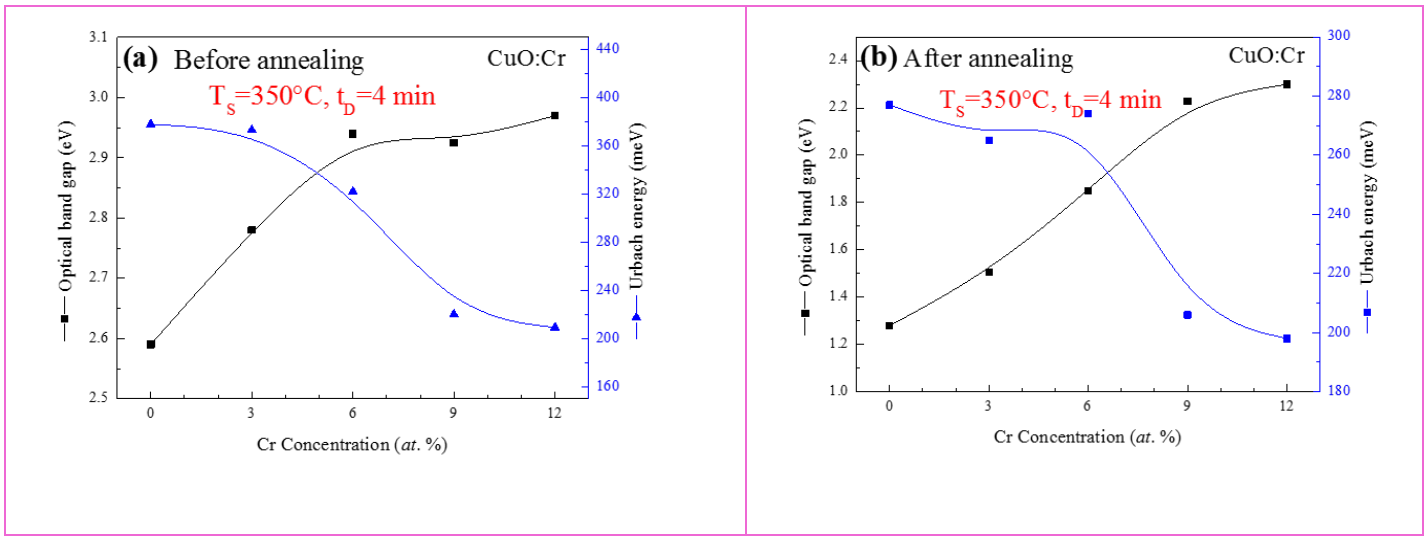


Figure III.8. Variation of optical band gap and Urbach energy of CuO:Cr thin films at different chromium concentrations **(a)** before annealing and **(b)** after annealing.

III.2.6. The effect of doping and annealing on the refractive index of CuO: Cr

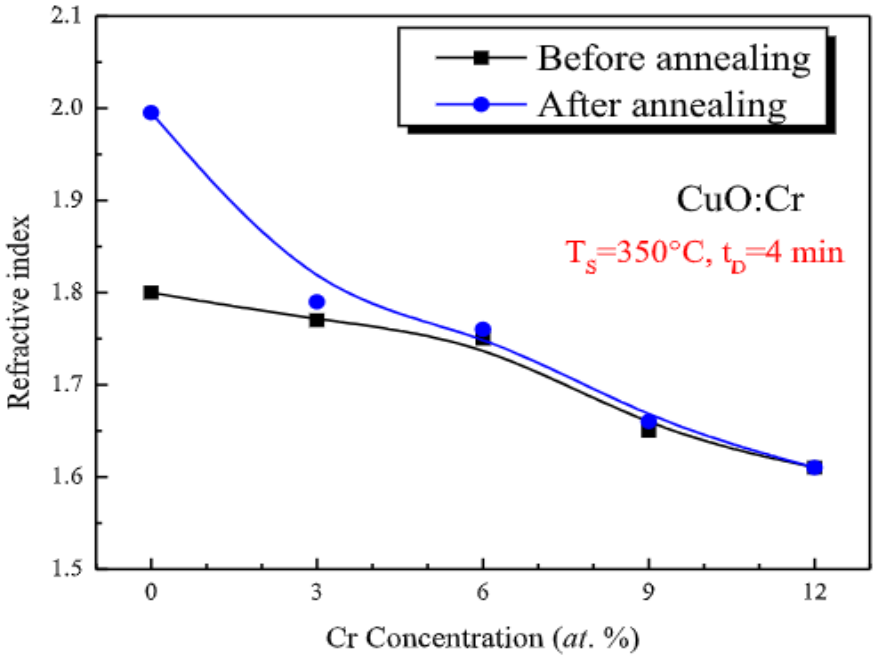


Figure III.9. The effect of doping and annealing on the refractive index of CuO: Cr.

Figure III.9 shows the variation of the refractive index of Cr-doped CuO thin films before and after annealing at 350°C for 1 hour. It is evident that the refractive index gradually decreases with increasing chromium concentration from 0 to 12 at.% in both cases, where the values decrease from approximately 2.0 to 1.6 before annealing and from 1.8 to 1.6 after annealing. This behavior is attributed to the increased porosity and oxygen content structure caused by chromium doping, which reduces the optical density of the films. This trend is consistent with what has been reported in the literature for CuO doped with other metals such as nickel[64].

It is also worth noting that the refractive index of chromium oxide (Cr_2O_3) is lower than that of copper oxide (CuO), due to the higher transparency of Cr_2O_3, which reinforces the observed decrease in refractive index with increasing chromium content.

On the other hand, the values obtained after annealing show a relative increase in the refractive index. This can be attributed to atomic rearrangement, improved crystallinity, and a reduction in structural defects, leading to a more uniform and compact film. During thermal treatment, the voids within the structure decrease or close, which reduces the transparency of the film and, in turn, decreases the speed of photon propagation within the material. Since the refractive index (n) is given by the relation:

$$n = \frac{c}{v} \qquad \text{(III.1)}$$

where c and v is speed of light in a vacuum and in the material, respectively.

The decrease in photon speed due to reduced voids results in an increase in the refractive index after annealing. It is important to note that the obtained values fall within the known refractive index range of copper oxide (1.5–3.5), indicating good agreement with the known optical properties of this material [5,64].

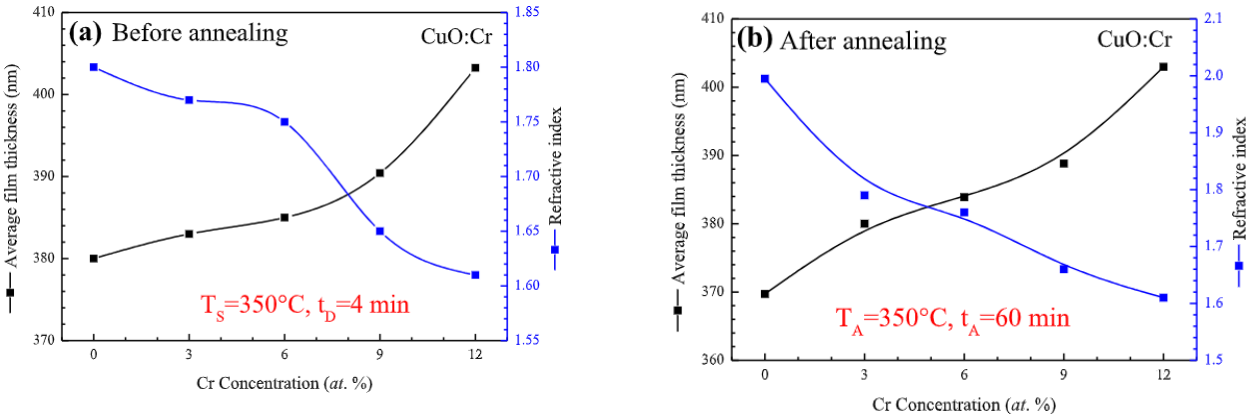


Figure III.10. Variation of average film thickness and refractive index of CuO:Cr thin films at different chromium concentrations before annealing **(a)** and after annealing **(b)**.

Figures III.10(a and b) show the relationship between average film thickness and refractive index as a function of chromium (Cr) concentration in copper oxide thin films before and after annealing. An inverse relationship was observed between thickness and refractive index, which is attributed to the increased porosity of the films. Higher porosity results in a thicker structure due to less cohesion of the material. At the same time.

III.3.Electrical characterizations

III.3.1. Effect of chromium doping and annealing on the electrical conductivity of Cu_xO

The electrical conductivity (σ) of Cu_xO:Cr thin films was measured using the four-point probe method. The current-voltage characteristics showed a linear relationship, indicating ohmic contact for all samples [7].

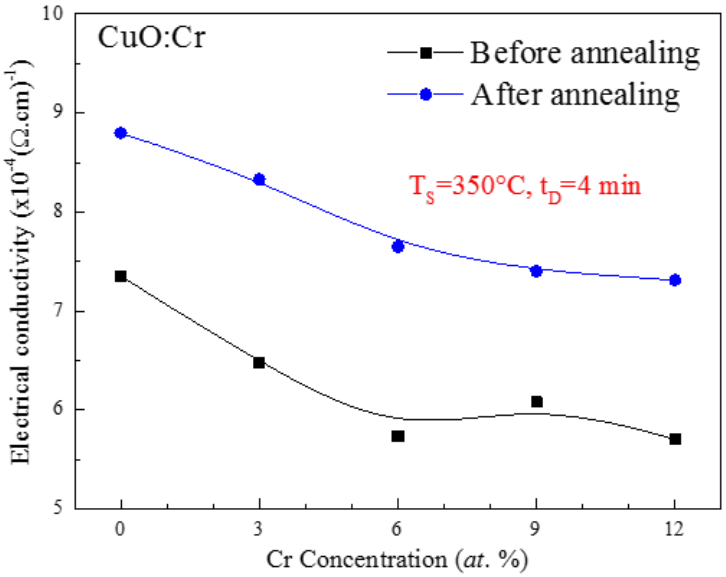


Figure III.11. Variation of electrical conductivity of CuO: Cr thin films as a function of Cr concentrations before and after annealing.

Figure III.11 shows the variation in electrical conductivity (σ) of Cu_xO:Cr thin films before and after annealing, as a function of chromium concentration. The films were prepared using the ultrasonic spray pyrolysis technique under identical deposition conditions. The variation in the electrical conductivity of CuO reveals that it is affected by chromium (Cr) concentration and annealing.

Before and after annealing, the electrical conductivity starts at a high value and gradually decreases as the Cr concentration increases. This decrease can be attributed to the effect of Cr impurities, which may reduce the number of charge carriers concentration (p). By annealing at 350°C for 1 hour, the electrical conductivity increased for all samples, indicating that the heat treatment enhanced the structural order, reduced internal defects, and increasing charge carriers concentration [61]. This aligns with the explanation in the text, which states that total conductivity follows the relation III.* that depending on the concentration and mobility of both electrons and holes. Therefore, the observed changes in conductivity are due to variations in these factors caused by doping and thermal treatment, highlighting the significant role of such processes in improving the electrical properties of doped metal oxide materials [96]:

$$\sigma = nq\mu_n + pq\mu_p \qquad \text{(III.2)}$$

where ; n and p are electron and hole carrier concentration, respectevely,

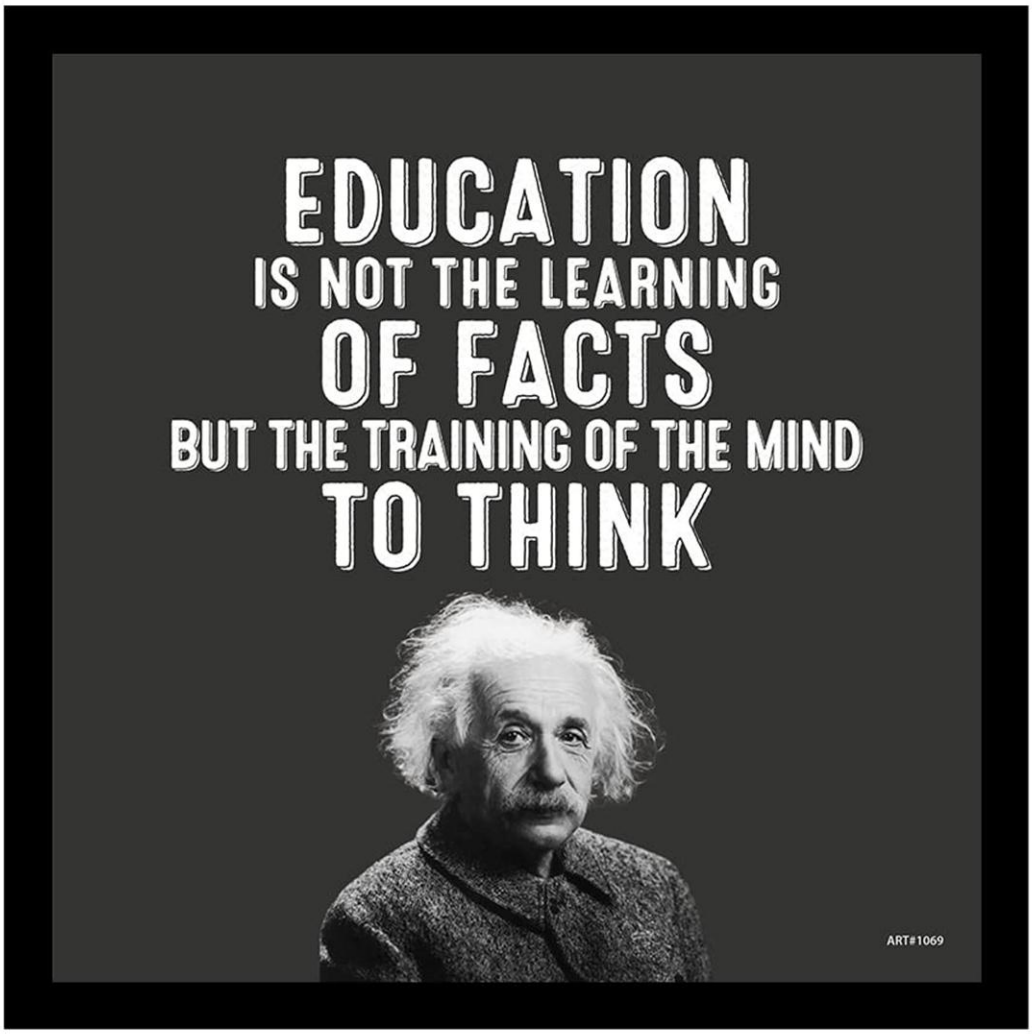
μ and μ : the mobility of charge carriers (electrons and holes), respectively,

q : the elementary charge of the electron.

On the other hand, the increases of electrical conductivity by annealing can be explained by the phase change from Cu_2O to CuO [97].

$$2Cu_2O + O_2 \xrightarrow{Heat} 4CuO \quad \text{(III.3)}$$

Conclusion



عادة المثل بعد الاهداء

General conclusion

This work aims to elucidate and investigate chromium-doped copper oxide (CuO:Cr) thin films deposited on glass substrates using the ultrasonic spray pyrolysis technique, in order to study the effect of doping percentage and annealing on the optical and electrical properties of these films.

In this study, we used the ultrasonic spray pyrolysis technique because of its simplicity, ease of implementation, and the fact that it does not require vacuum conditions. The thin films prepared using this technique are of high quality and exhibit excellent adhesion.

The CuO:Cr thin films were deposited at a fixed nozzle-to-substrate distance (5 cm) using an aqueous solution of copper (II) chloride dihydrate ($CuCl_2 \cdot 2H_2O$) and chromium (III) chloride hexahydrate ($CrCl_3 \cdot 6H_2O$) dissolved in water with different chromium doping levels (0 at. %, 3 at. %, 6 at. %, 9 at. %, and 12 at. %). The solution concentration (0.05 mol/l), deposition time (4 minutes), flow rate (60 ml/hr), and temperature were kept constant throughout the deposition process at 350°C.

The optical and electrical properties of the prepared samples were studied using UV-Visible-NIR spectrophotometry and the four-point probe technique to characterize the films' optical and electrical properties. This study led to the following conclusions:

With the increase in chromium doping percentage from 0 at. % to 12 at. %, it was observed that the optical transmittance was high in the visible range, ranging from 60% to 85% at the nozzle-to-substrate distance of 5 cm. The film thickness ranged from 380 to 400 nm before annealing and from 370 to 400 nm after annealing. Additionally, the optical band gap increased from 2.5 eV to 3 eV before annealing and from 1.2 eV to 2.3 eV after annealing. It was also observed that the Urbach energy decreased with increasing band gap energy, and that the refractive index decreased with increasing film thickness. The electrical conductivity of CuO decreased with increasing chromium percentage from 7.5×10^{-4} to 5.6×10^{-4} $(\Omega.cm)^{-1}$ before annealing, and from 8.9×10^{-4} to 7.5×10^{-4} $(\Omega.cm)^{-1}$. after annealing. These changes in the thin film properties are attributed to the increase in chromium doping and annealing, which lead to increased porosity and a reduction in structural defects caused by chromium atoms occupying appropriate sites and interstitial sites in the CuO lattice, making it less disordered.

References

References

[1] K. Limkrailassiri, Copper oxide by thermal oxidation for electrochemical cells and gas sensors, Thèse de doctorat, Université de California- Californie (2013).

[2] M. Dahrul, H. Alatas, Irzaman, Preparation and optical properties study of CuO thin film as applied solar cell on LAPAN-IPB Satellite, Procedia Environmental Sciences 33 (2016) 661–667

[3] P. Samarasekara, N.T.R.N. Kumara, N.U.S. Yapa, Sputtered copper oxide (CuO) thin films for gas sensor Devices, J. Phys: Condens. Matter 18 (2006) 2417–2420.

[4] D. Gopalakrishna, K. Vijayalakshmin, C. Ravidhas, Effect of annealing on the properties of nanostructured CuO thin films for enhanced ethanol sensitivity, Ceramics International 39 (2013) 7685–7691.

[5] SARI, Abir و BOUCHRIT, Sarra. élaboration et caractérisation des couches minces d'oxyde de cuivre non dopé. Mémoire de Master, Université Larbi Tébessi - Tébessa, Faculté des Sciences Exactes et des Sciences de la Nature et de la Vie, Département de Science de la Matière, 2017.

[6] M. Maache,Elaboration de films minces d'oxydes semiconducteurs par voie Sol-Gel. En vue d'application aux Optoélectroniques, capteurs et biomédicaux,Thèse de doctorat,Université Mohamed Khider de Biskra (2014).

[7] Menasria, N., & Talbi, H. Preparation and characterization of thin films of zinc-doped copper oxide (Master's thesis). Larbi Tebessi University - Tebessa, Faculty of Exact Sciences and Natural and Life Sciences, Department of Material Sciences(2017).

[8] F.Z. Ababsia & S. Fares, Élaboration et caractérisation des couches minces d'oxyde de nickel dopé au cuivre, Mémoire de master, Université Larbi Tébessi-Tébessa (2018).

[9] S. Agouram, Caractérisation de couches minces d'oxynitrures de chrome produites par pulvérisation cathodique réactive en présence d'air: influence de la vapeur d'eau contenue dans du plasma, Doctorate's Thesis, Namur University-Belgium (2003).

[10] Benmerad.R , Effect of Cr doping on optical and electrical properties of ZnO thin films deposited by spray pyrolysis technique, echahid cheikh larbi tebessi university of tebessa,2023

[11] J. Barnhart, Occurrences, uses, and properties of chromium, Regulatory Toxicology and pharmacology 26 (1997) 53-57.

References

[12] A. Allag, R. Saâd, A. Ouahab, N. Abdelmalek, B .Gasmi, Effect of solution concentration on the structural, optical andelectrical properties of SnO2 thin films prepared by spray pyrolysis, Optik 127 (2016) 2653–2658.

[13] M. Selma. H.A. Fadheela, H. Oleiwe, J.H. Khulaef, Preparation and characterization of tin oxide thin films by using spray pyrolysis technique, Tech Journal 33 (2015) 529- 538.

[14] H.A. Hamedani, Investigation of deposition parameters in ultrasonic spray pyrolysis for fabrication of solid oxide fuel cell cathodes, Doctoral Thesis, Georgia Institute of Technology (2008).

[15] حمية اكرام ، دراسة تاثير التطعيم على الخواص الضوئية للاغشية الرقيقة لاكسيد النيكل المطعم بالنحاس، جامعة قاصدي مرباح ورقلة ، (2021).

[16] K. Helaifa, Structural and opto-electrical study of SnO2 thin films elaborated by spray pyrolysis (home made), Echahid Hamma Lakhdar University-El-oued (2015).

[17] S. Redjel, N-H. Mekhaznia, Elaboration and characterization of tin oxide thin films deposited by spray pyrolysis, Master's thesis, Larbi Tebessi University-Tebessa (2020).

[18] S. Yahiaoui, L'effet de la molarité des différentes sources d'étain sur les propriétés des couches minces d'oxyde d'étain SnO_2 élaborées par Spray Ultrasonique, Magister Thesis, Mohamed Khider University – Biskra (2014).

[19] KHECHBA Mourad , Caractérisation de la réaction interfaciale entre une couche mince de tungstène et un substrat d'acier , UNIVERSITE MENTOURI-CONSTANTINE (2008).

[20] Yan-Mei Jiang, "Pulvérisation cathodique assistée par ordinateur", Thèse de doctorat, Université de Paris-Sud Centre d'Orsay (1992) .

[21] ح. مشرفي، دراسة الخصائص الكهربائية والبصرية لأغشية رقيقة لأكسيد الزنك (ZnO) المطعمة باللانثانوم (La) المحضرة بتقنية رشادة الانحلال الحراري، مذكرة ماستر، جامعة ورقلة، (2016).

[22] W.A. Bryant, The fundamentals of chemical vapour deposition, Journal of Materials Science 12 (1977) 1285- 1306.

[23] A. Richard, A.A. Durant. Les interactions ions énérgitiques-solides, édition INFINE.

[24] A. Rahal, " Elaboration des verres conducteurs par déposition de ZnO sur des verres ordinaires ", Thèse de Magister, Université d'El Oued, (2013).

[25]A. Douayar, "Contribution to the Study of the Structural, Optical, and Electrical Properties of Thin Films of Zinc Oxide (ZnO) Doped with Fluorine, Indium, Aluminum, and Neodymium," PhD Thesis, Mohammed V–Agdal University, (2013).

[26] M. Laagoun, Study of the effect of deposition time of nickel oxide (NiO) thin films on some physical properties (2017).

References

[27] K.Y. Rajpure, R.S. Pedanekar, S.K. Shaikh, Thin film photocatalysis for environmental remediation: A status review, Current Applied Physics 20 (2020) 931-952.

[28] D. Tainoff, "Influence of Defects on the Optical and Electronic Properties of ZnO Nanoparticles," PhD Thesis, Claude Bernard University Lyon 1, (2009).

[29] A. Benzagouta, "Effect of Stoichiometry on the Structural, Dynamic, and Electronic Properties of Si-C Systems: A Study by Molecular Dynamics," Doctoral Thesis, University of Constantine (2004).

[30] M. Djazair Bekacem, Study of the Optical and Electrical Properties of Doped Zinc Oxide Nanocrystals Deposited by Spray Pyrolysis, Master's Thesis, University of El Oued, (2014).

[31] مرادان، علي عايد. تكنولوجيا الأغشية الرقيقة وتطبيقاتها في الخلايا الشمسية. بحث بكالوريوس، جامعة بابل، كلية التربية للعلوم الصرفة، 2024.

[32] M. C. RAO , puldes laser deposition — ablation mechanism and applications , Journal of Modern Physics Conference Series Vol. 22 (2013) 355–360

[33] F Elaboration et caractérisation des films minces d'oxyde de titane pur.Labrèche, " et dopes Nd et Ag", thèse Doctorat, université de jijel,(2018).

[34] A. Thabet, Optimisation des conditions d'élaboration (température de substrat et distance bec-substrat) des films minces de ZnO par spray, Magister's Thesis, Mohamed Khider University-Biskra (2013).

[35] L. Herissi, Élaboration et caractérisation de couches minces d'oxydes métalliques destinées à des applications optoélectroniques, Doctorate's Thesis, Larbi Ben M'hidi University-Oum El Bouaghi (2016).

[36] B. Maatoub & S. Fissah, Study of the optical and electrical properties of tin oxide thin films deposited by spray pyrolysis, Master's Thesis, Larbi Tebessi University-Tebessa (2022)

[37] Marina Urbina ,Antonio Rinaldi, Santiago Cuesta-Lopez, Arcadii Sobetkii, Anca Elena Slobozeanu,Peter Szakalos, Yi Qin, Mythili Prakasam, Radu-Robert Piticescu,Cedric Ducros, and Alain Largeteau , The methodologies and strategies for the development of novel material systems and coatings for applications in extreme environments a critical review , manufacturing Rev. 5, 9 (2018)

[38] Samiha.R & Nour El houda.M , Elaboration and characterization of tin oxide thin films deposited by spray pyrolysis larbi tebessi university of tebessa (2019)

[39] Dr.asrar , Thin Film Deposition Technology 6_2019_05_23!10_16_06_AM.pdf

[40] L. yang, Caractérisation de couches minces de ZnO élaborées par la pulvérisation cathodique en continu, Thèse de doctorat, Université du Littoral cote d'opale-France (2012).

References

[41] K. Gupta, N. Kumar, J. R Laubscher, Conventional and advanced finishing of gears, Advanced Gear Manufacturing and Finishing, Ch.5 (2017) 127-165.

[42] C. Kelifi, Tin dioxide SnO2 thin films deposited by ultrasonic spray technique: Properties and applications, Doctoral Thesis, Mohamed Khider University, Biskra-2018.

[43] HAFDALLAH Abdelkader , Étude du Dopage des Couches Minces de ZnO Élaborées par Spray Ultrasonique , universite mentouri-constantine , (2007) .

[44] Dohare, Sameer. "Corrosion Protection and Modern Infrastructure." Introduction to Corrosion, IntechOpen, 16 June 2023. DOI: 10.5772/intechopen.111547.

[45] M. Othmane, Synthesis and characterization of Zinc Oxide (ZnO) Thin films deposited by spray pyrolysis for applying: electronics and photonics, Doctoral Thesis, Mohamed Khider University, Biskra-2018.

[46] A. Jilani, M. Shaaban, A. Wahab and A. H. Hammad, Advance Deposition Techniques for Thin Film and Coating , IntechOpen 33 (2017) 138-147.

[47] Saka, A., Gudata, L., Jule, L. T., Seeivasan, V., N., N., & Ramaswamy, K Synthesis of nano-sized lead sulfide thin films from Avocado (Glycosmis cochinchinensis) leaf extracts to empower pollution remediation. Scientific Reports, 12, 11710 , (2022)

[48] TEBANI hana , elaboration et caracterisation d'alliages ni-fe par electrodeposition , Université 8 mai 1945 Guelma , (2019) .

[49] Meke, A. S., & Dincer, I. Development and experimental investigation of a new direct urea fuel cell. International Journal of Hydrogen Energy, 88, 1123-1137 , (2024).

[50] H. Mualkia, "Élaboration Et Caractérisation De Couches Minces De Sulfure De Cadmium (CdS)", Thèse De Doctorat, Université Constantine, (2010).

[51] L.I. Popova, M.G. Michailov, V.K. Gueorguiev, A. Shopov, "Structure And Morphology Of Thin SnO_2 Thin Solid Films", Elsevier, Vol. 186, pp. 259–262, (1990).

[52]Hussein, K. I., Allehabi, S. O., Assem, E. E., Yousef, E. S., & Shaaban, E. R. Studying of cadmium oxide/Aluminium films for optoelectronics: Structural, optical and electrical characteristics. Inorganic Chemistry Communications, 162, 112191 (2024).

[53] lemouchi.w , effect of cu dopping on optical and electrical properties of ZnO thin film deposited by spray pyrolysis thechnique , Master's thesis, Larbi Tebessi University-Tebessa , (2022)

[54] R. Velmurugan, A. Incharoensakd, Nanoparticles and organic matter: Process and impact, Nanomaterials in Plants 1 (2018) 407-428.

[55] F. Bozon-Verduaz, Nanoparticles of metal and metal oxides: some peculiar synthesis methods, Brazilian Journal of Physics 39 (2009) 134-138.

References

[56]N. Kularatna, A. Steyn, R. Jayathu, F.S. James, Surge protection standards and practices, Design of Transient Protection Systems, Ch. 2 (2019)17-27.

[57] M. Lamri Zeggar, Cupric oxide thin films deposition for gassensor application, Thèse de doctorat, Université de Frères Mentouri-Constantine (2016). [57] M. Lamri Zeggar, Cupric oxide thin films deposition for gassensor application, Thèse de doctorat, Université de Frères Mentouri-Constantine (2016).

[58] A. Bejaoui, Capteurs à base des couches minces d'oxyde de cuivre (II) (CuO): optimisation et modélisation en vue de la détection de gaz, Thèse de doctorat, UniversitéAix Marseille & l'Université de Carthage-France & Tunisie (2013)

[59] مزنر امينة, M-ZnO (M : Cu, Ag) الزنك أكسيد مسحوق تحضير بأبعاد نانومترية واختبار نشاط التحفيز الضوئي له ;جيجل -جامعة محمد الصديق بن يحيى-(2022)

[60] S. Mehadjebi, La synthèse des nano poudres de CuO avec la méthode précipitation SolGel en utilisant le précurseur CuSO4 et l'étude de leurs propriétés structurales et optiques, Mémoire de magister, Université Mentouri-Constantine- Algérie (2015).

[61] Ahalapitiya H. Jayatissa, K. Kuo, Ambalapitiya C. Jayasuriya.Fabrication of cuprous and cupric oxide thin films by heat treatment. Applied Surface Science, 255: 9474–9479, 2009.

[62] A. Altaweel, Synthése de nanostructure d'oxyde de cuivre par microo-post- décharege microonde à pression atmosphérique, Thèse de doctorat, Université de lorraine (2014).

[63] T. Abdelaziz, Optimization des conditions d'élaboration (température de substrat et distancebec-substrat) des films minces de ZnO par spray, Thèse de Magister, Universite Mohamed Khider,Biskra, (2013).

[64] S. Guellati & C. Boussahla, Étude de l'effet de dopage par nickel et du recuit sur les propriétés des couches minces d'oxyde de cuivre, Master's Thesis, Larbi Tebessi UniversityTebessa (2019)

[65] E. Barrera-Calva, J.Méndez-Vivar, M. Ortega-López, L. Huerta-Arcos, J. Morales-Corona, R. Olayo-González, Silica-copper oxide composite thin films as solar selective coatings prepared by dipping Sol-Gel, Research Letters in Materials Science (2008) ID 190920 (5pp).

[66] Emeka charles nwanna, patrick ehi imoisili, sarah oluwabunmi bitire and tien-chien jen, biosynthesis and fabrication of copper oxide thin films as a p type semiconductor for solar cell applications , coatings 2021, 11, 1545

[67] S. Hettal, Optimization of the Concentration Of Copper Oxide Thin Films Elaborated By Pneumatic Spray, mémoire de master , Université Mohamed Khider -Biskra (2016-2017)

References

[68] Hachemi koucia mobarka & haddar nawel , l'influence du temps de dépôts sur les propriétés des couches minces de CuO élaborées par spray pneumatique, université mohamed khider de biskra, 2020

[69] عزوزة، أ. تحضير ودراسة أفلام رقيقة لأكسيد النحاس النقي (CuO) والمطعم بالسترونتيوم (Sr). مذكرة مقدمة لنيل شهادة الماستر في الفيزياء، تخصص فيزياء المواد، كلية العلوم الدقيقة والإعلام الآلي، قسم الفيزياء (2022).

[70] Emeka Charles Nwanna, Patrick Ehi Imoisili, Sarah Oluwabunmi Bitire and Tien-Chien Jen , Biosynthesis and Fabrication of Copper Oxide Thin Films as a PType Semiconductor for Solar Cell Applications , Department of Mechanical Engineering Science, Faculty of Engineering and the Built Environment,University of Johannesburg, Auckland, Johannesburg 2006, South Africa

[71] A. A. Ogwu, T.H. Darma, E. Bouquerel, Electrical resistivity of copper oxide thin films prepared by reactive magnetron sputtering, Journal of Achievements in Materials and Manufacturing Engineering, 24 (2007) 172–177.

[72] A. Bejaoui, Capteurs à base des couches minces d'oxyde de cuivre (II) (CuO): optimisation et modélisation en vue de la détection de gaz, Thèse de doctorat, Université Aix Marseille & l'Université de Carthage-France & Tunisie (2013).

[73] M. Lamri Zeggar, Cupric oxide thin films deposition for gas sensor application, Thèse de doctorat, Université Mentouri-Constantine- Algérie (2016).

[74] S. S. Shariffudin, S. S. Khalid, N. M. Sahat, M. S. P. Sarah, H. Hashim, Preparation and Characterization of nanostructured CuO thin films using Sol-gel Dip Coating, IOP Conf, Series: Materials Science and Engineering 99 (2015) 012007.

[75] جاء، ج. م. دراسة الخصائص البنيوية والضوئية لأغشية أكسيد النحاس (CuO). مذكرة تخرج مقدمة لنيل شهادة الماستر أكاديمي، جامعة الشهيد حمه لخضر بالوادي، كلية العلوم الدقيقة، قسم الفيزياء (2019).

[76] T. T. John, K. P. Vijayaknmar, C. S. Kartha, Y. Kashiwaba and T. Abe,"Effect of variation of Indium on structural and opticalproperties of IndiumSulfidethin films", IEE Explore, vol. 32, no. 9, P. 155 -157, (2009)

[77] خ. شدالة،" دراسة الخصائص الفيزئية للطبقات الرقيقة لأكسيد الزنك (ZnO) مطعمة ب (La) مرسبة بتقنيةالرش الكيميائي الحراري" مذكرة ماستر، جامعة قاصدي مرح، ورقلة، (2016).

[78] Dr. vinay kumar singh,thin film deposition by spray pyrolysis techniques, department of physics, raja singh college, siwan, bihar, india, pin-841226, 2017 jetir november 2017, volume 4, issue 11 www.jetir.org (issn-2349-5162).

[79] D. S. Albin, S. H. Risbud, "Nucleation and Growth Characteristics of Spray Paralyzed CdS Thin Films", Thin Solid Films, pp. 203–212, 1987.

[80] V.K. Singh, Thin film deposition by spray pyrolysis techniques, Journal of Emerging

References

Technologies and Innovative Research 4 (2017) 910.

[81] P.N. Onkundi, K.M. Munji, D.B. Bem, B. Muthoka, Effect of deposition parameters on optical and electrical properties of sno2:al thin films prepared by spray pyrolysis technique for optoelectronic devices, International Journal of Thin Films Science and Technology 7 (2018) 25-33.

[82] S. Lekshmy, SnO2 Thin films doped indium prepared by Sol-Gel method, Sol-Gel Science and Technology 67 (2013) 29-38.

[83] B. Abdallah, A. Ismail, H. Kashoua, and W. Zetoun, Effects of deposition time on the morphology, structure, and optical properties of PbS thin films prepared by chemical bath deposition, Journal of Nanomaterials 2018 (2018) 1826959

[84] A. Djelloul, Etude des propriétés morphologiques, structurales et optiques des couches de CdS, ZnS et CIS pour application cellules solaires de type métal/TCO/CdS/CIS, Doctoral Thesis, Mohamed Boudief University, Oran-2017.

[85] إ . لطيب ،" دراسة الخواص البنيوية المورفولوجية و الضوئية لأغشية أكسيد الزنك المطعمة لنيكل المحضرة بتقنية رذاذ الإنحلال الحراري " مذكرة ماستر أكاديمي ، جامعة ورقلة ، (2019) .

[86] رسالة ماجستر ,ادريس حمد , تحضير اكاسيد فلزية نانوية مختلفة بواسطة مستخلص نبات الكلغان ودراسة فعاليتها البايلوجية, كلية التربية ابن الهيثم جامعة بغداد , 2003

[87] M.M. Fahd, M. Rajab and S.M. Al-Abbas, Structural and optical characterization of Cr2O3 nanostructures: Evaluation of its dielectric properties 4 (2014) pp 027121-11.

[88] S. Tosgiyuki & L. Hong, Vacuum vaporization in the system MgO-Cr2O3, Journal of the American Ceramic society 61 (1978) 326-329.

[89] O. C. Rogojanu, G. A.Sawatzky & L. H. Tjeng, Stabilizing CrO by epitaxial growth, Groningen University-Netherlands (2002).

[90] على بعض الخصائص الفيزيائية." مذكرة (SnO_2) فرح الله منال. "تحضير ودراسة تأثير تطعيم أكسيد القصدير ماستر، جامعة محمد خيضر بسكرة، كلية العلوم الدقيقة وعلوم الطبيعة والحياة، قسم علوم المادة، (2023).

[91] X. Gao, Vanadium redox flow batteries for large-scale energy storage, Doctorat Thesis, Limerick University-Ireland (2012).

[92] C. Khelifi, Tin dioxide SnO2 thin films deposited by ultrasonic spray technique: Properties and Applications, Doctorate thesis, Med Khider University-Biskra (2018).

[93] B.D. Cullity, Éléments of X-ray Diffraction, Addition-Wesley Publishing Compagnie Inc., USA, 1978.

[94] Silan BATURAY1, Ilhan CANDAN1,2 , Cihat OZAYDIN3 , Structural, Optical and Electrical Characterizations of Cr-doped CuO Thin Films , 1 Dicle University, Faculty of Science, Department of Physics, 21280, Diyarbakir, Turkey 2 Dicle University, Institute of

References

Science and Technology, Department of Physics, 21280, Diyarbakir, Turkey 3 Department of Computer Engineering, Faculty of Engineering, University of Batman, 72100, Batman, Turkey

[95] K. Derrar, M. Zaabat, A. Hafdallah, N. Rouabah, b. Gasmi, I. Zerrouk, Optical and structural properties of SnO2 thin films deposited by spray pyrolysis technique: effect of solution concentration, Defect and Diffusion Forum 397 (2019) 179-186.

[96] R. Bacha, La synthèse des nano particules de CuO avec la méthode de précipitation Sol-Gel, en utilisant le précurseur CuCl2, et l'étude de leurs propriétés structurales et optiques, mémoire de magister, Université de Mentouri-Constantine (2015).

[97] U.C. Bind, R.K. Dutta, G.K. Sekhon, K.l. Yadav, J.B.M. Krishna, R. Menon, P.Y. nabhiraj, Ion implantation induced phase transformation and enhanced crystallinity of as deposited copper oxide thin films by pulsed laser deposition, Superlattices and Microstructures 84 (2015) 24–35

Abstract

Effect of Cr doping on optical and electrical properties of CuO thin films deposited by spray pyrolysis technique

Abstract

This research aims to study the effect of chromium doping on the optical and electrical properties of copper oxide thin films prepared using the spray pyrolysis technique. Copper oxide thin films are considered promising materials for various applications in optoelectronic and thermoelectric devices. Doping with elements such as chromium can effectively enhance their optical and electrical properties, making them suitable for different technological applications such as gas sensors, solar cells, and display devices.

In this work, thin films of copper oxide doped with chromium (CuO:Cr) were fabricated at different doping levels (0 at. %, 3 at. %, 6 at. %, 9 at. %, and 12 at. %) on glass substrates using spray pyrolysis and thermal decomposition techniques. Solutions of copper chloride and chromium chloride were used to prepare the necessary solutions. During the preparation, specific conditions were maintained, such as substrate temperature and evaporation rate, to ensure the formation of homogeneous films.

The results showed that increasing the chromium concentration significantly affected the films's properties. where the bandgap increased and the optical absorption decreased with higher chromium doping levels. Additionally, the study demonstrated that the doped CuO:Cr films exhibited good electrical conductivity, making them suitable for various applications.

It is worth noting that factors such as solution concentration, thermal treatment, and the substrate play a significant role in enhancing the films' properties. Overall, the study concluded that doping with chromium is an effective method to improve the performance of copper oxide thin films by controlling the preparation conditions and chromium concentration to achieve the best optical and electrical properties.

Keywords: CuO:Cr thin films, Spray pyrolysis, Nozzle-substrate distance, band gap, Urbach energy, electrical conductivity.

Abstract

Effet du dopage au Cr sur les propriétés optiques et électriques des couches minces de CuO déposées par la technique de pyrolyse par pulvérisation

Résumé

Cette recherche vise à étudier l'effet du dopage au chrome sur les propriétés optiques et électriques des couches minces d'oxyde de cuivre préparées par la technique de spray pyrolyse. Les couches minces d'oxyde de cuivre sont considérées comme des matériaux prometteurs pour diverses applications dans les dispositifs optoélectroniques et thermoélectriques. Le dopage avec des éléments tels que le chrome permet d'améliorer efficacement leurs propriétés optiques et électriques, les rendant ainsi adaptées à différentes applications technologiques comme les capteurs de gaz, les cellules solaires et les dispositifs D'affichage.

Dans ce travail, des couches minces d'oxyde de cuivre dopées au chrome (CuO:Cr) ont été fabriquées avec différents niveaux de dopage (0 % at., 3 % at., 6 % at., 9 % at., and 12 % at.) sur des substrats en verre en utilisant les techniques de spray pyrolyse et de décomposition thermique. Des solutions de chlorure de cuivre et de chlorure de chrome ont été utilisées pour préparer les solutions nécessaires. Pendant la préparation, des conditions spécifiques telles que la température du substrat et la vitesse d'évaporation ont été maintenues afin d'assurer la formation de films homogènes.

Les résultats ont montré qu'une augmentation de la concentration de chrome influençait de manière significative les propriétés des films, la bande interdite augmentant et l'absorption optique diminuant à mesure que la concentration en chrome augmentait. De plus, l'étude a montré que les films dopés CuO:Cr présentaient une bonne conductivité électrique, ce qui les rend adaptés à diverses applications.

Il convient de noter que des facteurs tels que la concentration de la solution, le traitement thermique et le type de substrat jouent un rôle important dans l'amélioration des propriétés des films. Globalement, l'étude a conclu que le dopage au chrome est une méthode efficace pour améliorer les performances des couches minces d'oxyde de cuivre en contrôlant les conditions de préparation et la concentration de chrome, afin d'obtenir les meilleures propriétés optiques et électriques.

Mots clés : Couches minces de CuO:Cr, Spray pyrolyse, distance bec substrat, Bande interdite, Energie d'Urbach, Conductivité électrique.

Abstract

تأثير التشويب بالكروم على الخواص البصرية والكهربائية لأغشية أكسيد النحاس الرقيقة المترسبة بتقنية التحلل الحراري بالرش

الملخص

يهدف هذا البحث إلى دراسة تأثير تطعيم الكروم على الخصائص البصرية والكهربائية للأغشية الرقيقة من أكسيد النحاس، والتي جرى تحضيرها باستخدام تقنية الرش الحراري. تعتبر أغشية أكسيد النحاس الرقيقة من المواد الواعدة لتطبيقات متنوعة في الأجهزة الكهروضوئية والكهروضوحرارية. ويعد تطعيمها بعناصر مثل الكروم وسيلة فعّالة لتحسين خصائصها الضوئية والكهربائية، ما يجعلها مناسبة للتطبيقات التقنية المختلفة مثل المستشعرات الغازية والخلايا الشمسية وأجهزة العرض.

في هذا العمل، تم تصنيع أغشية رقيقة من أكسيد النحاس المطعمة بالكروم (CuO:Cr) بنسب مختلفة (0%، 3%، 6%، 9%، 12%) على ركائز زجاجية باستخدام تقنية الرش الحراري والانحلال الحراري. استُخدمت محاليل من كلوريد النحاس وكلوريد الكروم في تحضير هذه الأغشية. خُصصت ظروف التحضير، مثل درجة حرارة الركيزة وسرعة التبخير، لضمان الحصول على أغشية متجانسة.

أظهرت النتائج أن زيادة تركيز الكروم أثرت بشكل واضح في خصائص الأغشية؛ إذ زادت فجوة الطاقة وانخفض الامتصاص البصري مع ارتفاع تركيز الكروم. كما بينت الدراسة أن أغشية CuO:Cr أظهرت ناقلية كهربائية جيدة، ما يؤهلها لتطبيقات متعددة.

تجدر الإشارة إلى أن عوامل مثل تركيز المحلول، والمعالجة الحرارية، ونوع الركيزة تلعب دورًا مهمًا في تحسين خصائص الأغشية. بشكل عام، خلص البحث إلى أن تطعيم أكسيد النحاس بالكروم يعتبر طريقة فعالة لتحسين أداء الأغشية الرقيقة من خلال التحكم في ظروف التحضير ونسب الكروم لتحقيق أفضل الخصائص البصرية والكهربائية

الكلمات المفتاحية: الأغشية الرقيقة من(CuO:Cr) ، الرش بالانحلال الحراري، المسافة بين الفوهة والركيزة، فجوة